High Compression Ratio Turbo Gasoline Engine Operation Using Alcohol Enhancement

by

Raymond Lewis

B.S. Mechanical Engineering
Massachusetts Institute of Technology, 2011

Submitted to the Department of Mechanical Engineering in Partial Fulfillment of the Requirements for the Degree of

MASTER OF SCIENCE IN MECHANICAL ENGINEERING

AT THE

MASSACHUSETTS INSTITUTE OF TECHNOLOGY

SEPTEMBER 2013

Signature of Author .....
Department of Mechanical Engineering
August 19, 2013

Certified by.....
John B. Heywood
Sun Jae Professor of Mechanical Engineering, Emeritus
Thesis Supervisor

Accepted by.....
David E. Hardt
Ralph E. & Eloise F. Cross Professorship of Mechanical Engineering
Chairman, Department Committee on Graduate Students

High Compression Ratio Turbo Gasoline Engine Operation Using Alcohol Enhancement

by Raymond Lewis

Submitted on August 19, 2013

Submitted to the Department of Mechanical Engineering in Partial Fulfillment of the Requirements for the Degree of Master of Science in Mechanical Engineering

Abstract

Gasoline – ethanol blends were explored as a strategy to mitigate engine knock, a phenomena in spark ignition engine combustion when a portion of the end gas is compressed to the point of spontaneous auto-ignition. This auto-ignition is dangerous to the operation of an internal combustion engine, as it can severely damage engine components. As engine designers are trying to improve the efficiency of the internal combustion engine, engine knock is a key limiting factor in engine design.

Two methods have been used to limit engine knock that will be considered here; retarding the spark timing and addition of additives to reduce the tendency of the fuel mixture to knock. Both have drawbacks. Retarding spark reduces the engine efficiency and additives typically lower the heating value of the fuel, requiring more fuel for a given operating point.

To study this problem a turbocharged engine was tested with a variety of combinations of gasoline and ethanol, an additive with very good anti-knock abilities. Pressure was recorded and GT Power simulations were used to determine the temperature within the cylinder. An effective octane number was calculated to measure the ability of the fuel to resist knock. Effective octane numbers varied from 91 for UTG91 to 111 for E25, respectively.

Engine simulations were used to extrapolate to points that couldn't be tested in the experimental setup and generate performance maps which could be used to predict how the engine would act inside of a vehicle. It was found that increasing the compression ratio from 9.2 to 13.5 leads to a 7% relative increase in part load efficiency. When applied in a vehicle this leads to a 2-6% increase in miles per gallon of gasoline consumption depending on the drive cycle used. Miles per gallon of ethanol used were significantly higher than gasoline; 141 miles per gallon of ethanol was the lowest mileage over all cycles studied.

Thesis Supervisor: John B. Heywood
Title: Sun Jae Professor of Mechanical Engineering, Emeritus

(This page was intentionally left blank)

Table of Contents

Acknowledgements

First, I would like to thank Professor Heywood for taking me on as a graduate student on this project, and for giving me guidance and support throughout the course of this project. His knowledge, patience and advice helped me a great deal as I worked on this project.

Next I would like to thank the administrative staff, both at the Sloan Automotive Laboratory and at the Mechanical Engineering Graduate Office for helping to ensure the work went as smoothly as possible.

Finally I would like to thank friends and family for their continuing encouragement and understanding.

Abbreviations

BMEP: brake mean effective pressure

CR: Compression Ratio

E10: 10% ethanol and 90% gasoline by volume

E20: 20% ethanol and 80% gasoline by volume

E25: 25% ethanol and 75% gasoline by volume

E50: 50% ethanol and 50% gasoline by volume

E85: 85% ethanol and 15% gasoline by volume

HWFET: Highway Fuel Economy Test Driving Cycle

MBT: maximum brake torque

RON: Research Octane Number

UDDS: Urban Dynamometer Driving Cycle

US06: supplemental driving cycle

UTG91: regular test hydrocarbon gasoline, 91 RON octane

UTG96: premium test hydrocarbon gasoline, 96 RON octane

1. Introduction

A recent trend in internal combustion engine design has been towards increasing the efficiency of the engine. This is largely due to the fact that the price of gas is extremely variable and mileage, a measure of how much gasoline is consumed by the engine is often a selling point used to market vehicles. Strategies used to improve the efficiency of internal combustion engines, include increasing the compression ratio and using a turbocharger.

Both strategies can be used to increase the efficiency in different ways. Increasing the compression ratio increases the pressure inside the cylinder, which increases the work that can be done over a given cycle with the same initial conditions. A turbocharger compresses the air inside the cylinder, allowing for more air to be fed in. This leads to an increase in the available output power, because more air means more fuel is available to combust. The relative magnitude of efficiency loss mechanisms decrease with increased turbocharging, so as a result, the engine becomes more efficient. [1]

While both approaches improve the efficiency of an internal combustion engine, an added disadvantage in spark ignition engines is the increase in the tendency of an engine to undergo engine knock. Engine knock is a phenomenon in an internal combustion engine, in which the pressure and temperature of unburned gas reach a point where it spontaneously ignites.

Typical combustion in a spark ignition engine can be modeled as a flame front beginning at the spark plug during spark ignition and continuing through the cylinder as more of the fuel-air mixture is combusted. As the flame propagates the combustion products expand, compressing the unburned gas. In some situations, the pressure and temperature of the unburned gas becomes high enough to ignite on its own. This causes shock waves which can severely damage the engine.

Knock is typically most prevalent when operating a high loads and low speeds. High loads, measured by the applied torque of the engine, correspond to high cylinder pressures and temperatures which increase the tendency of a fuel to knock. Lower speeds mean longer combustion times, and therefore more time to knock for a given operating point.

Preventing and/or limiting engine knock is a key limiting factor in improving the efficiency of internal combustion engines. Increasing the compression ratio of an engine will increase the pressure inside of it, promoting knock. Likewise, turbocharging will also increase the pressure inside of the cylinder, promoting knock.

How much an internal combustion engine performance can safely be improved is limited by how much engine knock can occur in the cylinder. Therefore in order to achieve improvements in efficiency using these methods, engine knock must be mitigated.

1.1. Ethanol Blends

In order to limit the tendency of fuel to knock additives are typically added. Examples of fuels that have been used to limit knock are ethanol, methanol and water. Adding such fuels contributes two separate effects which can limit engine knock. First, these additives increase the fuel chemical octane number. Second, the heat of vaporization of such fuels is much higher than gasoline. As the fuel is injected as a liquid and vaporized within the cylinder a higher heat of vaporization will lead to cooler air in the cylinder. As a result of this charge cooling effect, the mixture in the cylinder will be cooler, which lower its tendency to knock.

Ethanol has received particular consideration because of its potential as a carbon neutral alternative to gasoline, as well as its use as a knock resistant fuel. However, while it has been demonstrated as an effective anti-knock fuel it has several drawbacks. Ethanol has a lower heating value that is significantly lower than typical gasoline. As a result, more fuel is required for the same energy output when using ethanol, and other alcoholic additives.

One possibility which will be explored here is that of using two tanks, one with gasoline and one with a knock resistant additive, in this case, ethanol. Such a configuration could enable the engine to run on typical gasoline when not in regions where there is a risk of knock and add ethanol from an auxiliary tank when operating in regimes where there is a high risk of knock. As the tendency of a certain fuel to knock is increased, so is the amount of ethanol added to it.

1.2. Spark Retard

Another, more common method to reduce engine knock in the engine is with spark retard. The goal behind spark retard is to delay the ignition at the spark plug so that the fuel does not have enough time to reach auto-ignition. This is because spark retard decreases the pressures in a given engine, and makes the peak pressure point within the cylinder occur later in the cycle. Both these effects decrease the tendency for knock to occur at a certain condition.

Doing this however decreases the efficiency of the engine. The reason this occurs is because the work produced by the gas in the cylinder is equal to the integral of pressure times the differential change in volume:

$$W = \int PdV$$

Retarding the spark makes peak pressure occur later in the combustion/expansion stroke and decreases its magnitude, lowering the output power.

This leads to another tradeoff. Spark retard would allow higher loads with the same fuel, decreasing the relative amount of knock resistant additives but at the same time would decrease the efficiency, requiring more energy, and as a result, more fuel, altogether.

2. Experimental Methods

A 2.0L Turbocharged Ecotec Engine was used for experimental measurements. This engine had a compression ratio of 9.2, a total displacement volume of 2 Liters and a twin-scroll turbocharger. The experimental plan was to run the engine at speeds of 1500 rpm to 3000 rpm at various loads. In this way a performance map could be generated by recording MBT at every point in the operating range. At each point a spark sweep was performed, during which the spark timing was advanced or retarded as much as possible, subject to performance constraints.

While running the experiments several limits were imposed on the range of loads applicable to the engine. First, the maximum pressure within the cylinder was not allowed to surpass 100 bars. Any higher pressures, given the high loads the engine would be subject to, would risk blowing the cylinder head gaskets. This was done by retarding the spark with respect to MBT. While this strategy decreased the efficiency it also enabled the engine to be run at higher loads. Second, the exhaust temperature was kept below 950 C. This was the limit of the temperature range of the current turbocharger. When this constraint was reached, the spark was advanced.

Two types of gasoline were used as a baseline: a 91 RON octane, similar to normal gasoline and a 96 RON 'premium' octane. To consider the effect of blending ethanol, the 91 RON octane gasoline was mixed with ethanol. Blends of 91 RON were done because the goal of this research was to quantify the antiknock benefits of ethanol, which would be more noticeable if compared with a lower octane gasoline. Also, 91 RON is closer to the type of gasoline consumers currently use. Mixtures were done on a by volume basis and will be referred to by the ethanol percentages, by volume. Mixtures tested are E0, E10, E20, E25, E50 and E85.

2.1. Defining Knock Onset

When running the engine, knock onset could be determined by the audible noise it makes but when analyzing the data a more rigorous approach was taken by using the pressure trace. Because knock manifests itself as high frequency pressure oscillations a filtered pressure trace was used to determine the point at which knock occurs. The steps used to determine knock onset are as follows.

Pressure data was taken in the cylinder at a sampling frequency of 100 kHz. A Fast Fourier Transform was then performed in MATLAB for every cycle. This converts the pressure trace from the time domain into the frequency domain. Second, anything corresponding to a frequency below 2 kHz or above 50 kHz was removed. 50 kHz was chosen as an upper limit to eliminate aliasing. 2 kHz was chosen as a lower limit to eliminate noise and any changes in the cylinder not related to engine knock. This was essentially a band pass filter.

An inverse Fast Fourier Transform was applied to the filtered signal to return to the time domain and the largest value of each cycle was recorded. This value was named the knock intensity for

each cycle. Knock onset was defined as the following two conditions met; the largest knock intensity was between 2 bar and 4 bar and the percent of cycles with a knock intensity greater than 1 bar (the knock frequency) was higher than 10%. An example of a cycle where knock onset has occurred is shown in Figure 1.

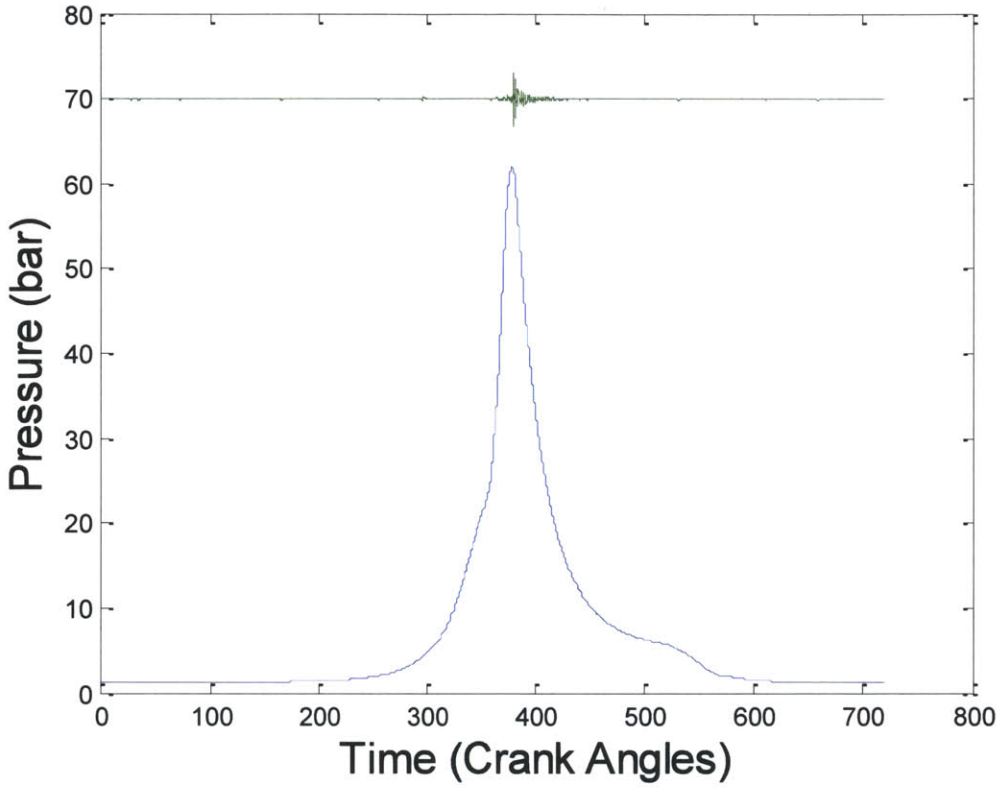

Figure 1: A sample case of how knock is measured. Pictured here are a smoothed pressure trace (blue) and the high pass filtered knocking data used to measure knock onset (green).

3. Simulation Tools

The experimental setup was only used to test the engine in a small component of the entire performance range. In order to consider cases beyond what could be run in the experiment, and to explore how the engine will behave in a vehicle, two simulation programs were used; GT Power and Autonomie.

3.1. GT Power

Most of the constraints mentioned here could be relaxed by the use of knock additives and stronger engine components, and the engine operating range extends much farther than what is tested. The engine tested can reach speeds below 1000 rpm and above 6000 rpm. This is beyond the limits of our experimental setup so in order to obtain results for situations outside of our experimental range, GT Power was used.

GT Power is a simulation package specifically designed for the study of internal combustion engines. A model of the engine was provided by colleagues at GM (the manufacturer of the engine we used) and used to get results for situations beyond our ability to run experimentally. Using this simulation tool it was possible to create a performance map for the engine over the entire operating range.

The performance map was expressed as a graph. Speed was on the x-axis, BMEP was on the y-axis and a contour of brake fuel conversion efficiency was superimposed on the graph. BMEP was chosen because it was a measure of the work available from the engine that is independent of the engine size.

$$\mathrm{BMEP} = \frac{\mathrm{Pn}}{V_D N} = \frac{2\pi \mathrm{Tn}}{V_d}$$

Here P is the power produced by the engine, N is the speed T is the torque, n is the number of revolutions per cycle (2 in this case because this was done with a four stroke engine) and V_D is the displacement volume. The displacement volume is the volume the cylinders of the engine sweep in one stroke; 2 Liters for this engine.

3.1.1. Burn Rate

The models used required the burn rate inside of the cylinder. This was calculated from experimental data assuming that combustion in the cylinder could be modeled using two zone poly-tropic processes; expansion of burned species and compression of unburned species.

$$V = V_u + V_b = V_{uo}\left(\frac{P_o}{P}\right)^{\frac{1}{n_u}} + V_{bf}\left(\frac{P_f}{P}\right)^{\frac{1}{n_f}}, V_{bf} = x_b V_f, V_{u0} = (1 - x_b)V_0$$

Here x_b is the fraction of fuel burned V is the (time dependent) volume of the cylinder P is the cylinder pressure, V_u and V_b are the volume of the burned and unburned fuel mixtures, P_0 and P_f are the initial and final pressures, V_0 and V_f are the initial and final volumes and V_{bf} and V_{u0} are intermediate variables. The poly-topic exponents, n_u and n_f, are calculated using the slope of log-log fits of the pressure v volume curve before combustion begins, and after it finished respectively.

Using these equations to solve for x_b in terms of values which can be measured leads to the equation below:

$$\frac{\left(V(P)^{\frac{1}{n_u}} - V_0(P_0)^{\frac{1}{n_u}}\right)}{\left(P^{\left(\frac{1}{n_u}-\frac{1}{n_f}\right)}V_f(P_f)^{\frac{1}{n_f}} - V_0(P_0)^{\frac{1}{n_u}}\right)} = x_b$$

This equation was solved for each case and fed into GT Power, which was then used to simulate the performance of the engine. The initial and final states, denoted by the subscripts 0 and f are the points of ignition, i.e. spark, and the opening of the exhaust valve.

3.1.2. Variables in the Simulation

The GT Power simulation allowed for a wide range of variables that can be adjusted to modify conditions in the engine. In order to match simulations with results several variables were adjusted. These included heat transfer to the cylinders, fraction of fuel burned during the cycle, amount of charge cooling used to cool the fuel-air mixture etc.

Heat Transfer: GT Power has several built-in heat transfer models for calculating the heat transfer from the fuel-air mixture to the cylinder walls. The models used typically underestimate the heat transfer to the environment and therefore a scaling factor was included to adjust how much heat transfer actually occurs. A scaling factor of 1.1 to 1.4 is typically recommended as a beginning approach. After matching experiments to data it was determined that values between 1 and 1.2 are accurate.

Fraction of Fuel Burned: Combustion efficiency is not unity in the cylinder, and as a result, not all of the fuel inside of the cylinder is ignited during the combustion phase. Typical values of combustion efficiency for current engine range between 93% and 97%. Experimentally it was found that 95% generates a good match between theory and experiment.

Charge Cooling: When injected into the cylinder, the fuel is a liquid which vaporizes in the cylinder, cooling anything it comes in contact with. Ideally the fuel should only cool the mixture but a fraction of the fuel will come in contact with, and by evaporation, cool the cylinder walls. How much this occurs is beyond the scope of this study. To provide a bench mark, this question was studied by colleagues at GM using a proprietary CFD model of engine evaporation in the engine cylinder. This work was done as part of a previous study at base boost at 2000 rpm. [2] They found that, irrespective of the fraction of ethanol within the cylinder, thirty percent of the charge cooling effect available via the evaporating fuel was absorbed by the cylinder walls, leaving seventy percent to cooling the mixture. This was kept consistent throughout the tests conducted here.

3.1.3. Comparison of GT Power with Experimental Results

In order to validate the GT Power model's ability to simulate real world test conditions GT Power was used to simulate conditions run in the experimental engine. The most extensively tested fuels were gasoline (UTG96) and E85.

E85: The most extensively tested fuel was E85, chiefly because it yielded the best anti-knock benefit of all the fuels tested. A performance map done using GT Power data was shown in Figure 2. What can be seen here is that at low loads the efficiency increases quickly with load, but at high loads it stagnates. This is due to the peak pressure constraints, seen in detail in Figure

3. Here peak pressure is plotted as a function of NIMEP. At the low load points, there is a closely linear relationship between load and pressure, but at the high load points the pressure constraint leads to a leveling off, as spark is retarded to avoid exceeding 100 bars.

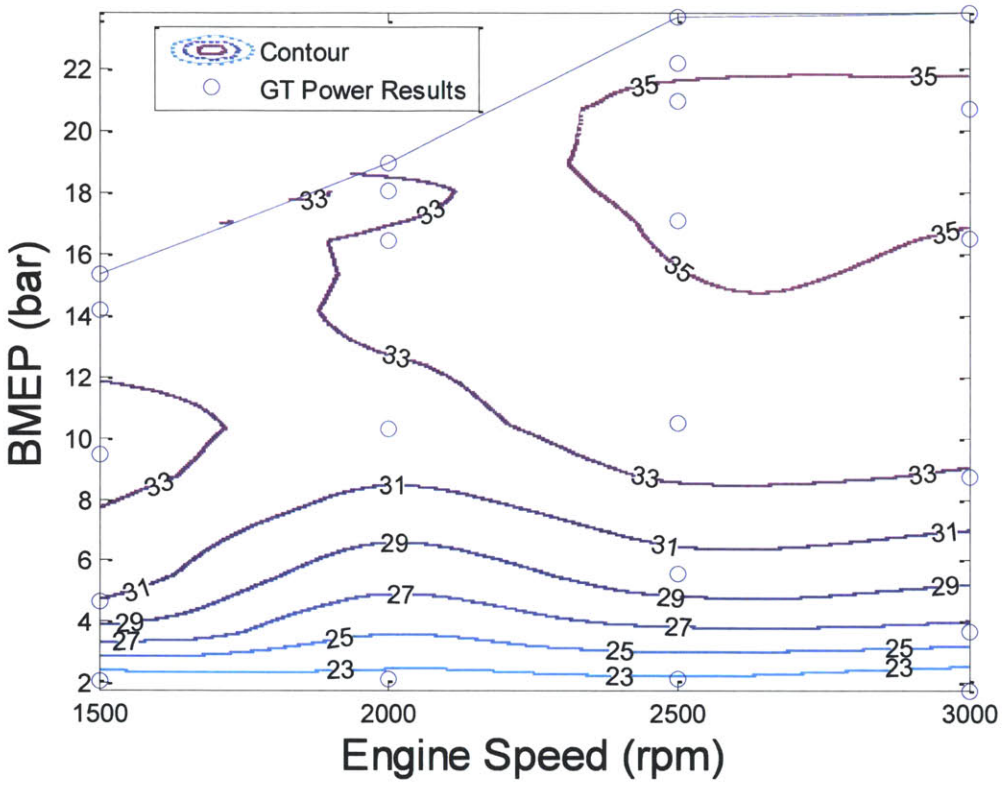

Figure 2: GT Power simulation of the experimental performance map for E85.

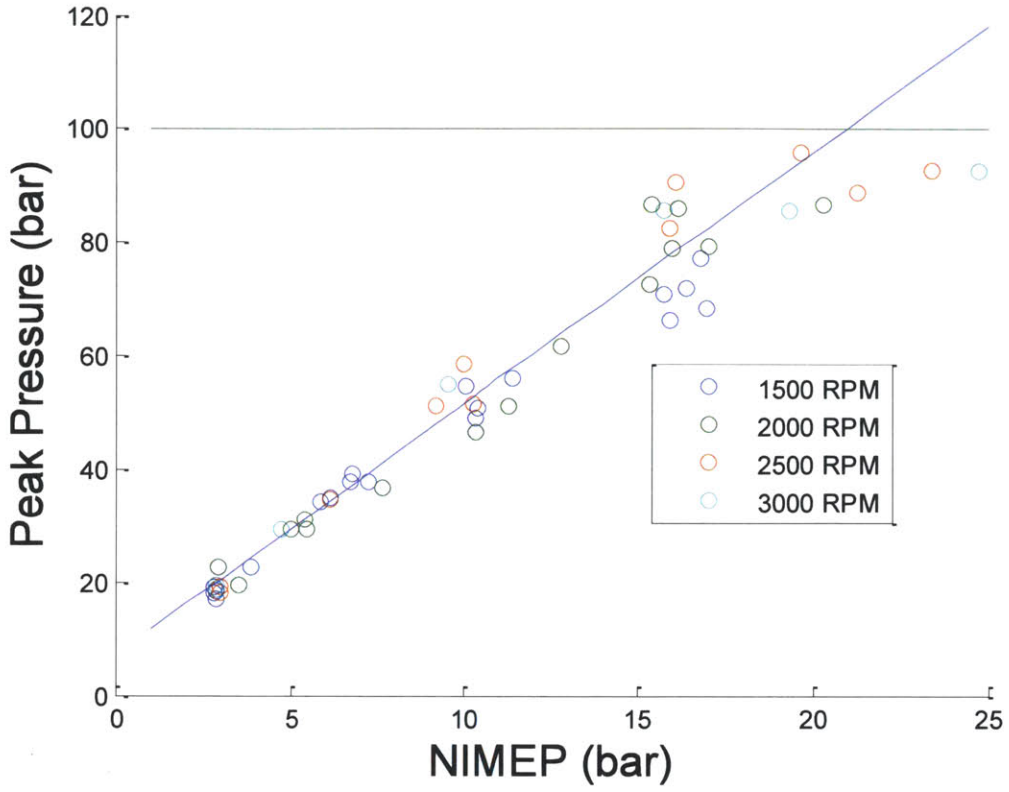

Figure 3: Peak Pressure at highest load timing for cases done using E85. A linear fit of peak pressure v. NIMEP for data below the peak pressure limitation is shown, as is the peak pressure limit. Note that peak pressure levels off as the peak pressure limitation is reached.

Comparisons of GT Power with the experiment at different speeds are shown in Figures 4-7. The simulation and experiment are in close agreement here, which validates the model and parameters chosen as accurate for simulating engine conditions.

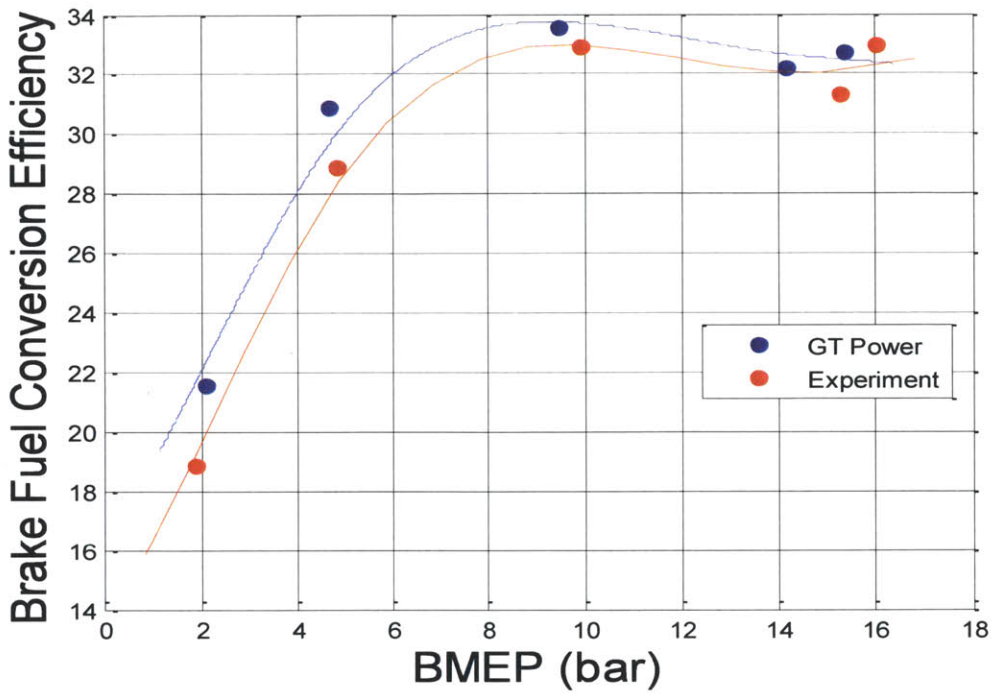

Figure 4: Ethanol Brake Fuel Conversion Efficiencies at 1500 RPM

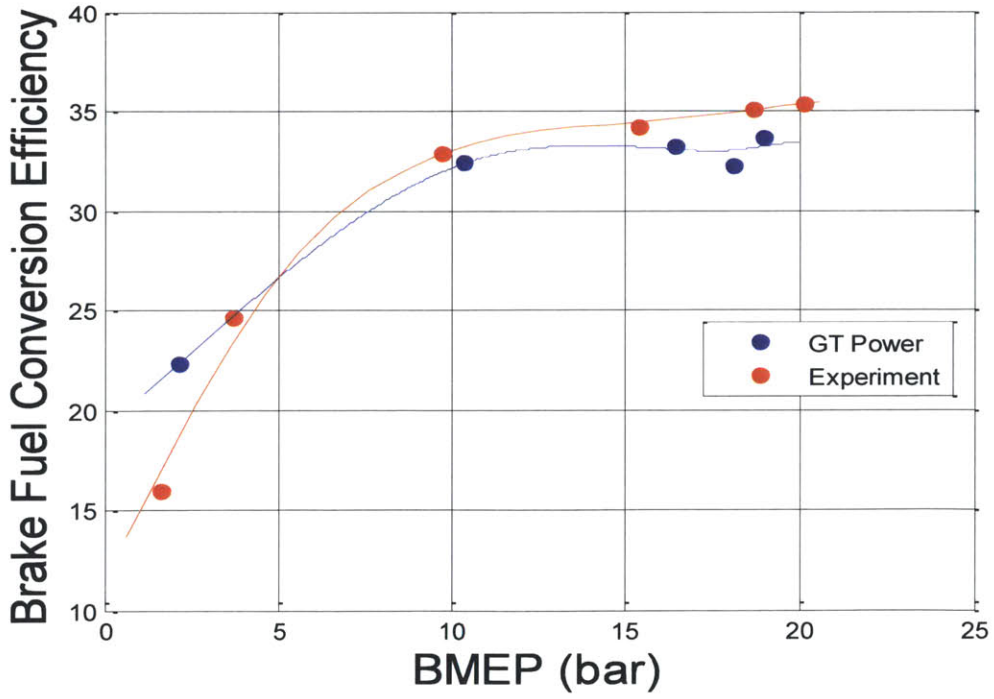

Figure 5: Ethanol Brake Fuel Conversion Efficiencies at 2000 RPM

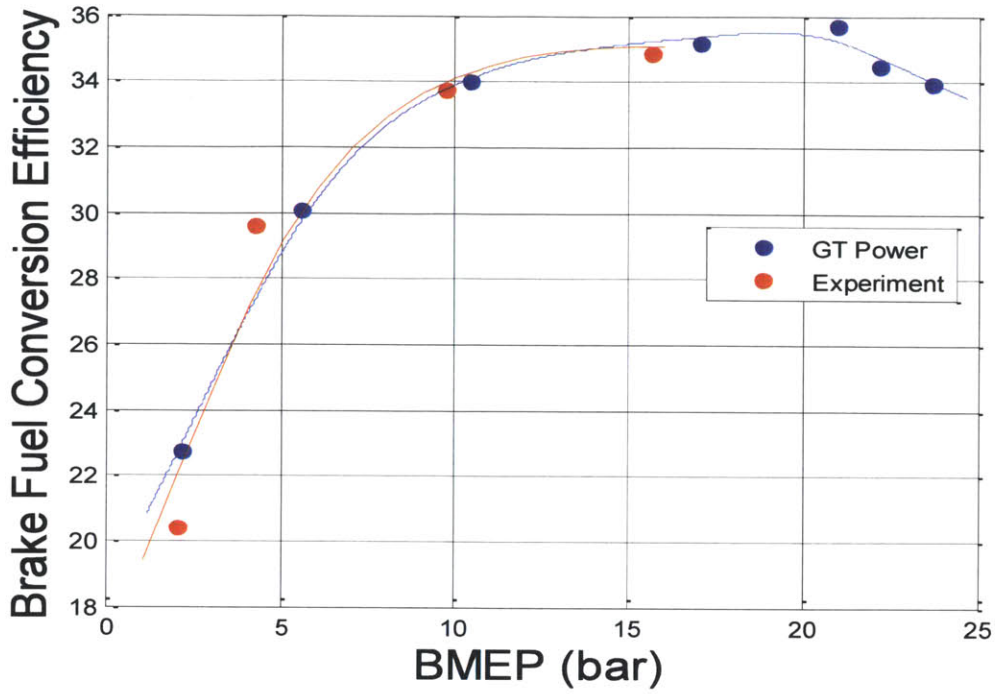

Figure 6: Ethanol Brake Fuel Conversion Efficiencies at 2500 RPM

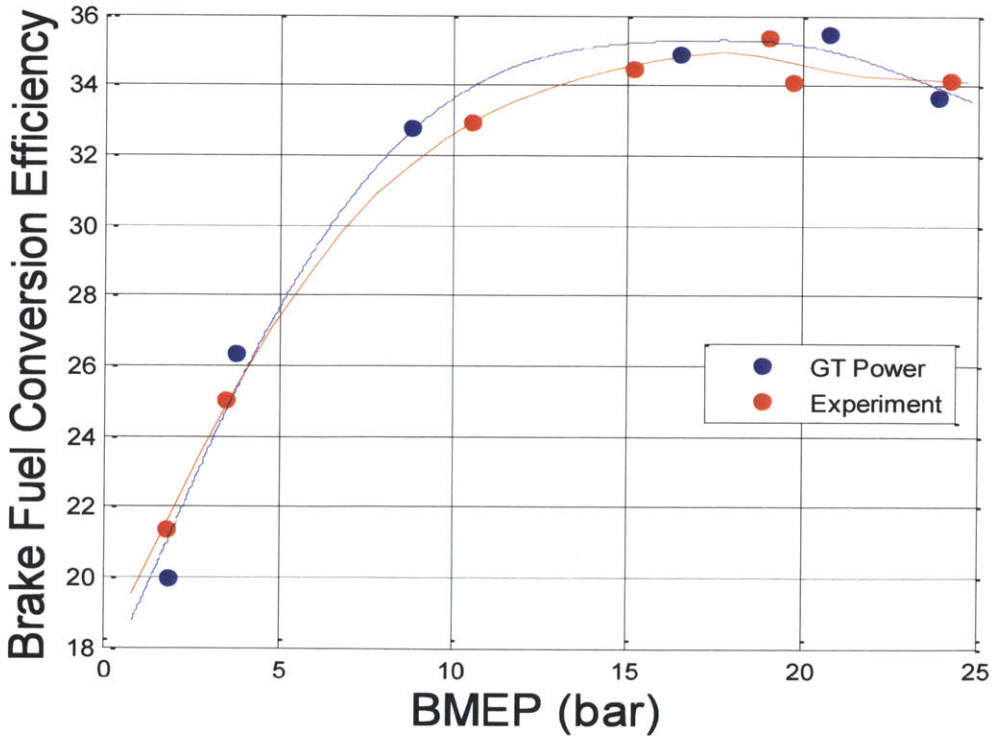

Figure 7: Ethanol Brake Fuel Conversion Efficiencies at 3000 RPM

UTG96: Premium gasoline was also tested at a wide enough range to generate a performance map, shown in Figure 8. Being a gasoline it was more susceptible to knock than the higher ethanol blends. As a result the highest loads tested here were much lower than initially used with E85. A comparison of GT Power with experiment was shown in Figures 9-12.

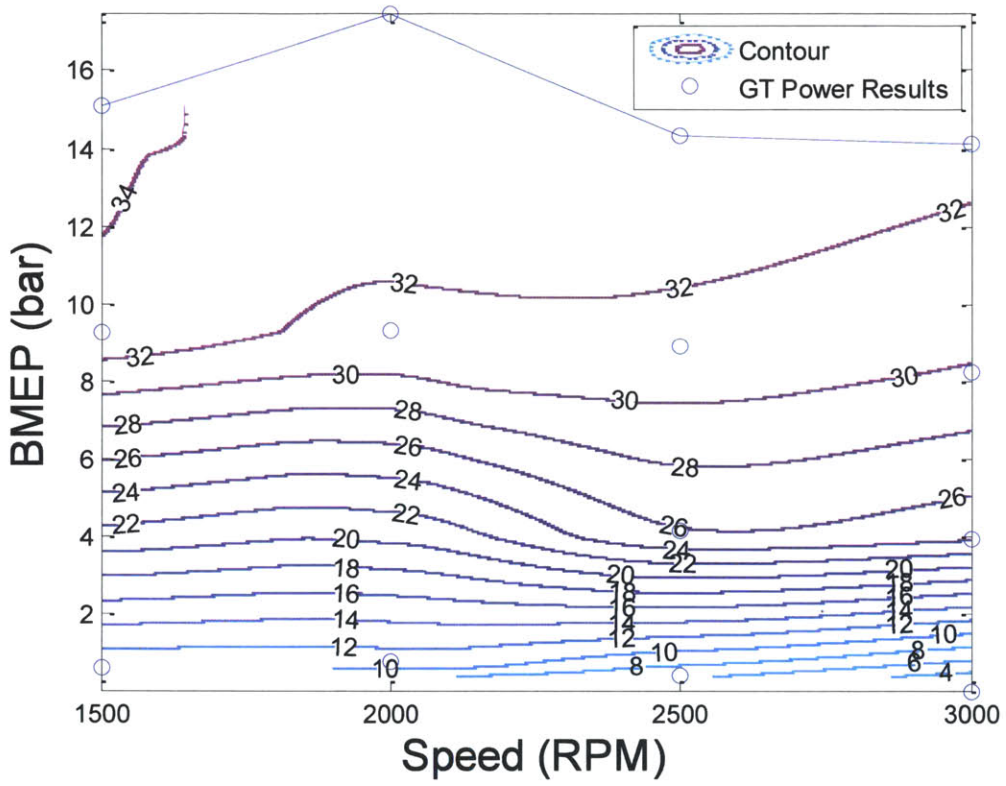

Figure 8: Turbocharged 2L DI Engine Performance Map Simulated in GT Power with UTG96 gasoline.

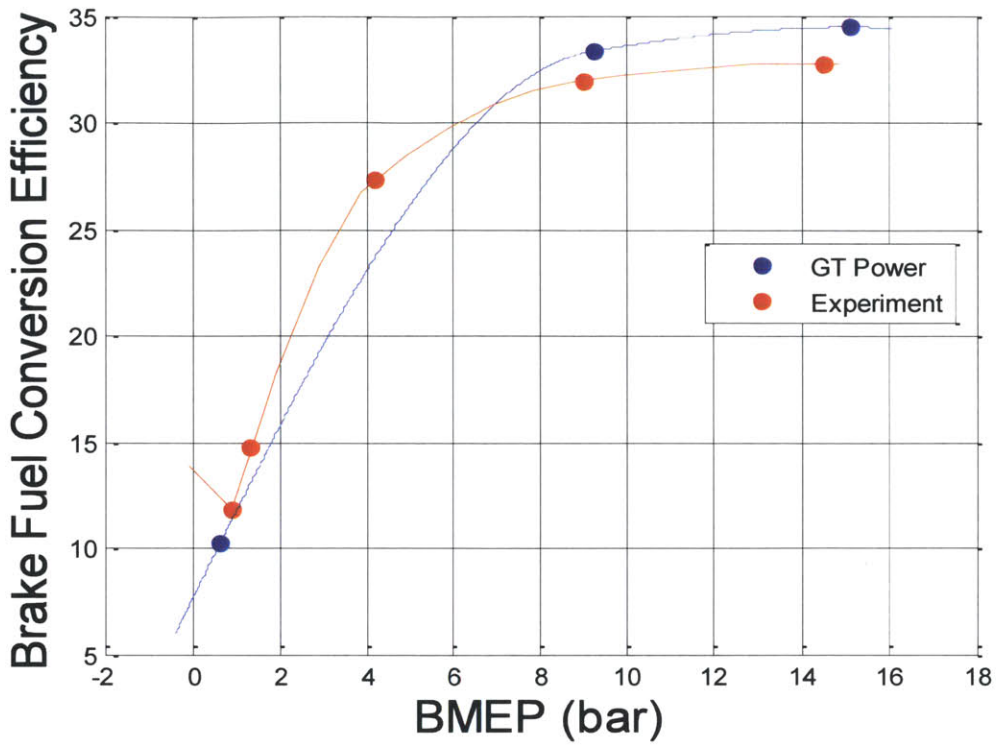

Figure 9: UTG96 at 1500 RPM

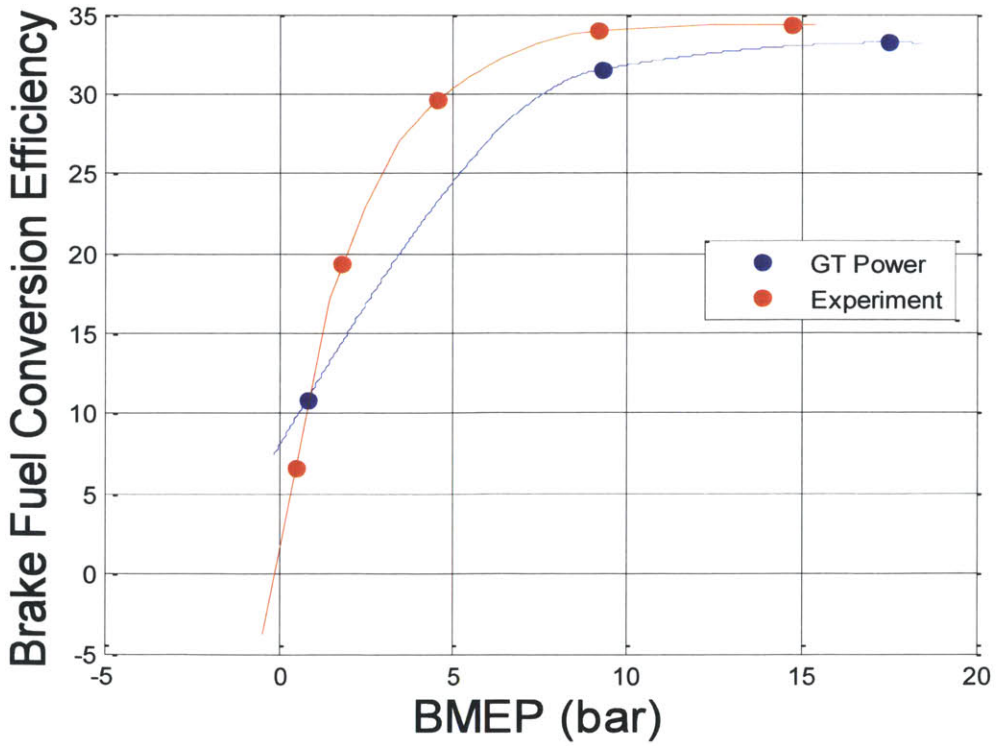

Figure 10: UTG96 at 2000 RPM

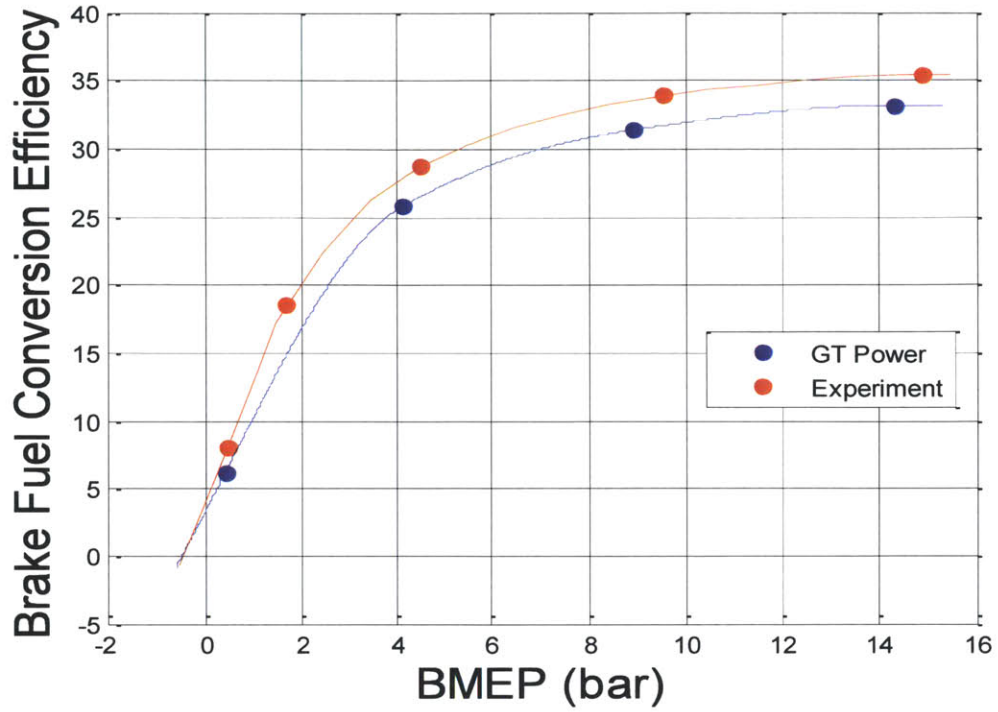

Figure 11: UTG96 at 2500 RPM

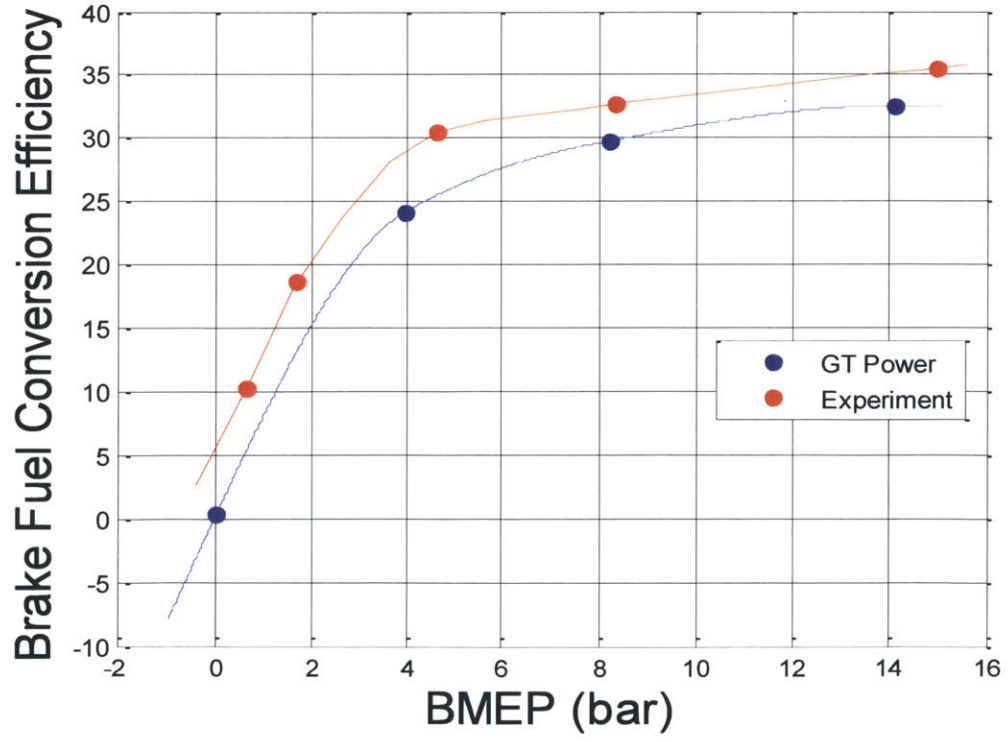

Figure 12: UTG96 at 3000 RPM

3.1.4. Fuel Comparison

A comparison of brake fuel conversion efficiencies was done for the fuels tested at low loads to determine how the engine behaves under MBT conditions. At high loads the fuel dependent constraints due to knock lead to a deviation from MBT timing. As a result high load behavior varies significantly from fuel to fuel. At low load fuel characteristics were expected to be similar. Results of efficiency v. BMEP were shown in Figures 13-16.

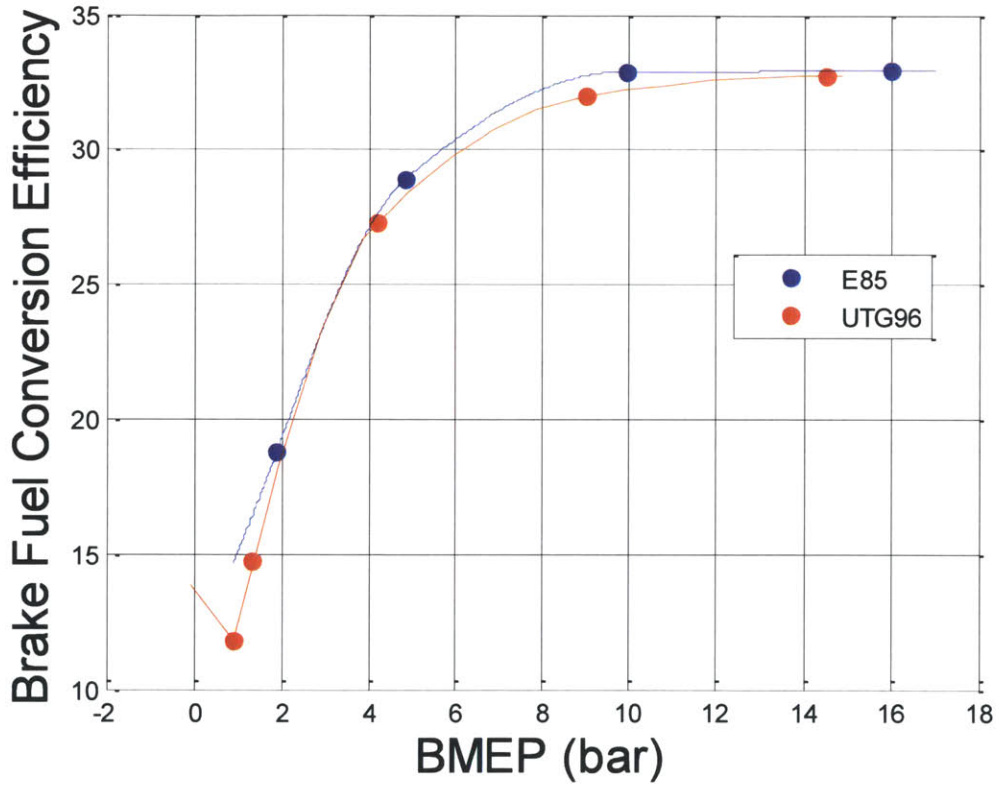

Figure 13: Fuel Comparison at 1500 RPM

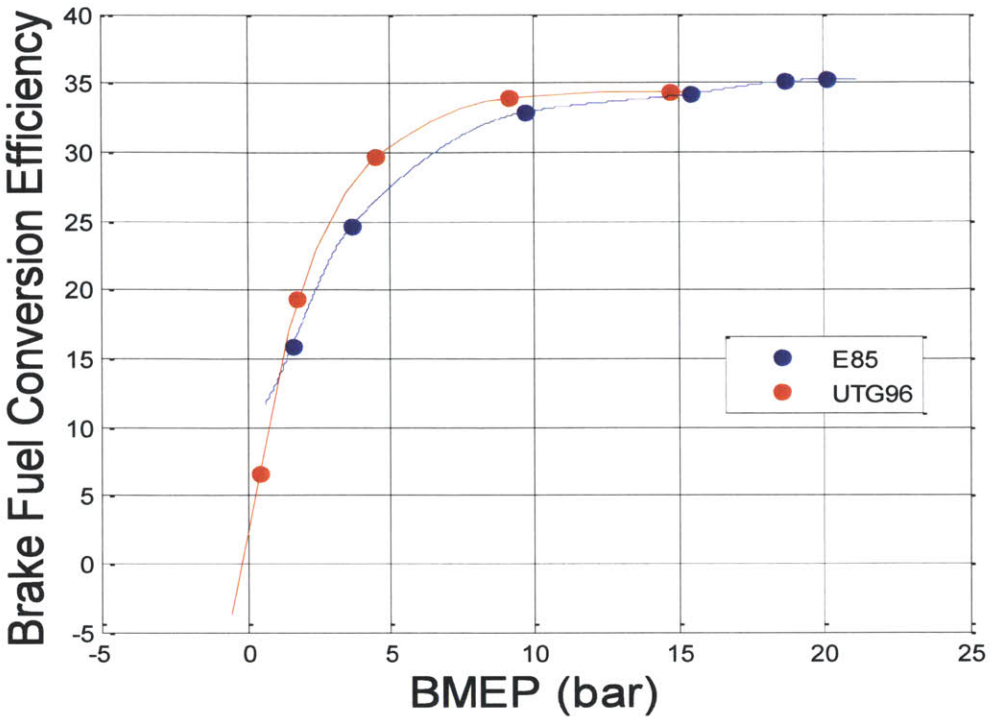

Figure 14: Fuel Comparison at 2000 RPM

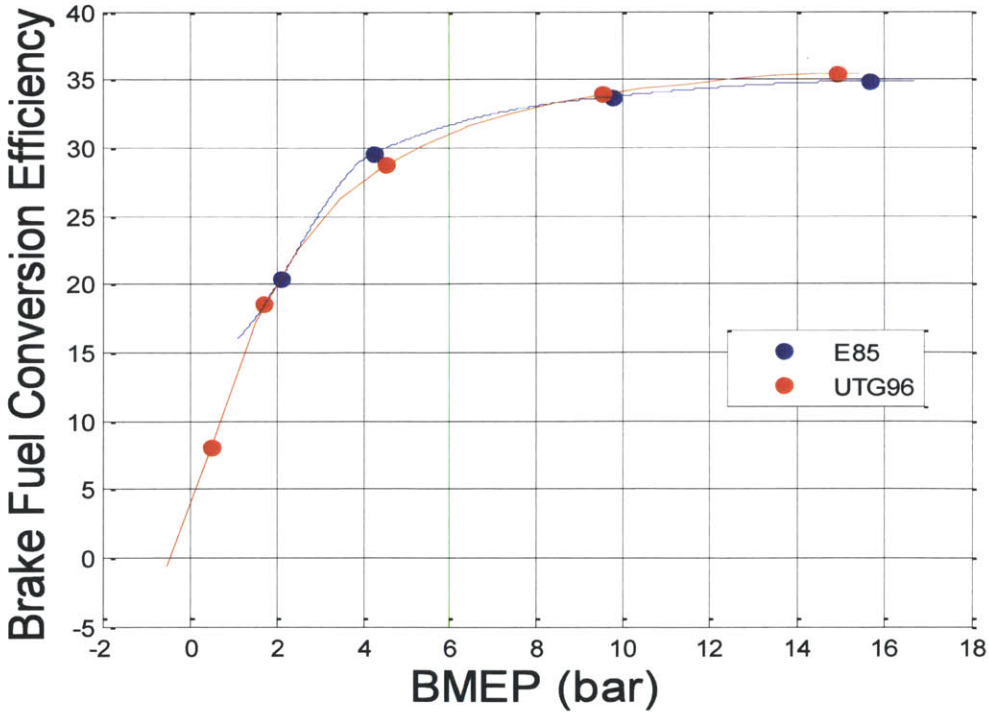

Figure 15: Fuel Comparison at 2500 RPM

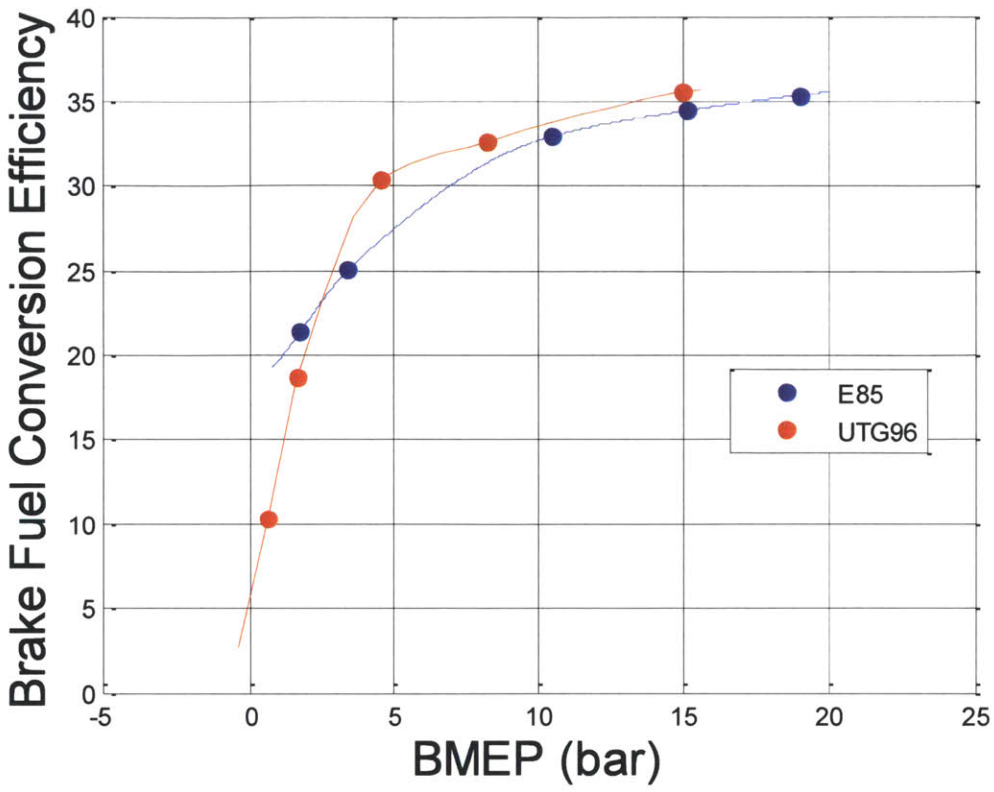

Figure 16: Fuel Comparison at 3000 RPM

These results show the brake fuel conversion efficiency as a function of load for the different fuels. It was determined from these data that efficiency is essentially independent of fuel as a first order approximation.

4. Evaluating Anti-Knock Properties – The Knock Integral Approach

In order to compare the effectiveness of each fuel at preventing knock an "effective" octane number was developed using a model for Auto-ignition. It is assumed that the reaction can be modeled as a one – step chemical reaction. In this case the reaction was modeled as a one step Arrhenius reaction with a time constant τ. At each point in the cycle the reaction can be said to progress by an amount equal to:

$$\int \frac{dt}{\tau} = 1$$

Knock onset can be said to occur when the value of this integral reaches 1. The correlation used in this investigation is as follows. [2]

$$\tau = 17.68 \left(\frac{ON}{100}\right)^{3.402} p^{-1.7} \exp\left(\frac{3800}{T}\right)$$

Here τ is in milliseconds, ON is the effective octane number, P is the cylinder pressure in bars and T is the temperature of the unburned mixture in Kelvin. By defining knock onset as the point where the value of the integral reaches 1 an octane number can be found for each fuel.

Results for the UTG96 gasoline are shown below. Pressure and temperature are shown in Figure 17 and the knock integral evaluated at different trial octane numbers is shown in Figure 18. The auto-ignition integral was a definite integral evaluated between two bounds, beginning of compression and knock onset. Beginning of compression was set to the intake valve closure. Knock onset was first assumed to occur at either peak pressure or peak temperature. Both were tested here. More details are shown in the table. Shown are the crank angle and the octane number where this induction/ auto-ignition time integral reached a value of one.

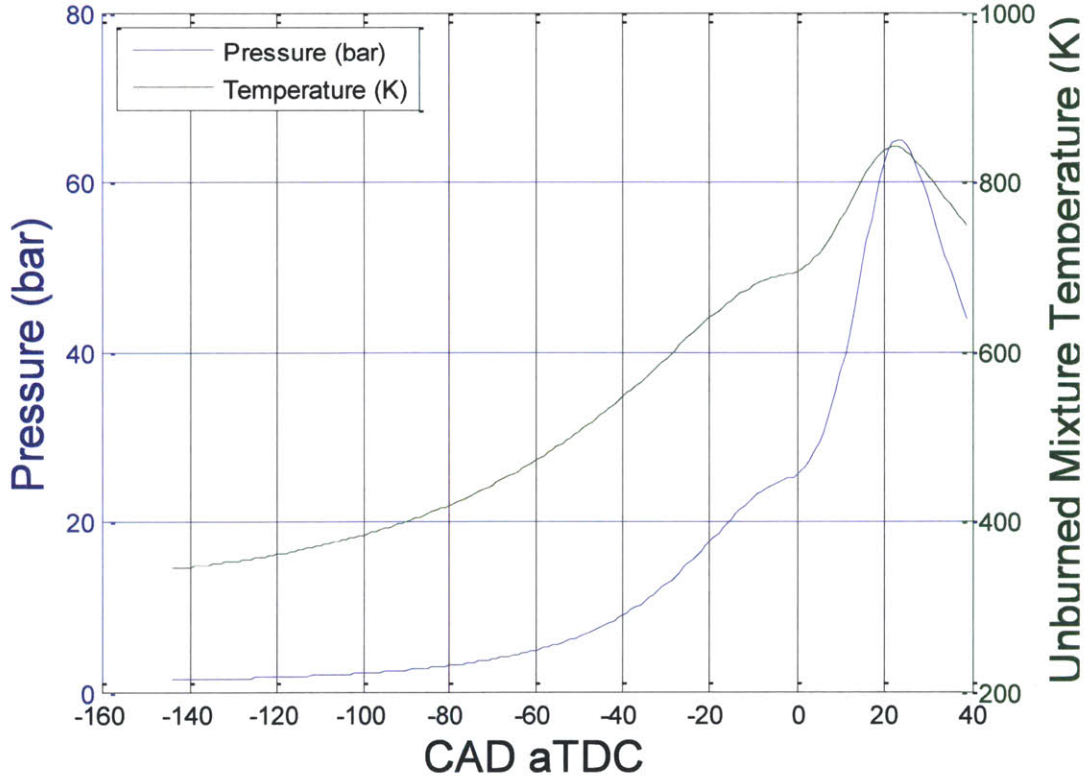

Figure 17: In cylinder Unburned Mixture Temperature and Pressure plotted versus crank angle degrees after TDC

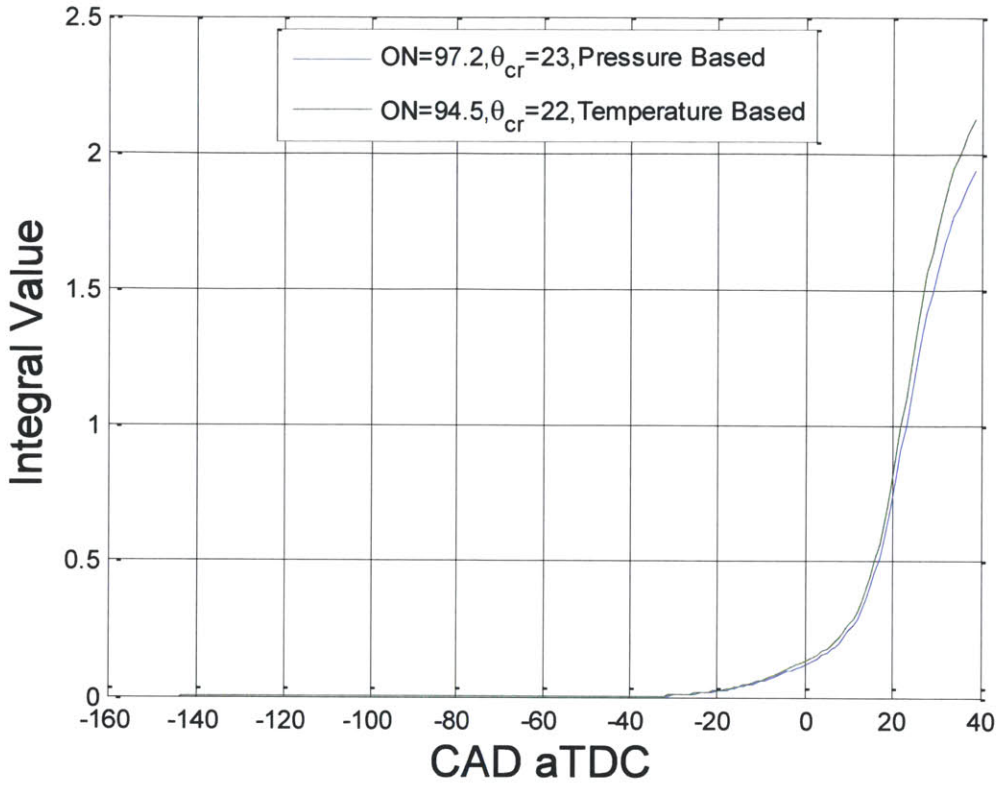

Figure 18: Auto-ignition Integral Value assuming that knock onset (i.e. the value of the auto-ignition integral approaching 1) occur at peak pressure and peak temperature

Table 1: Comparison of Different Auto-ignition Octane Numbers, found using peak pressure and peak temperature as the points of knock onset

Maximum Pressure		**Maximum Temperature**		**Fuel Spec Sheet**
Crank angle ATDC (deg)	Octane Number	Crank angle ATDC (deg)	Octane Number	Octane Number
23	**97.2**	22	94.5	**97.1**

Maximum pressure was reached slightly later than the maximum unburned mixture temperature so the estimated octane number using maximum pressure is slightly higher. It also is closer to the value given on the fuel specification sheet, so maximum pressure was used for future results.

The calculations for Figures 19-20 and Table 2 were done for a mixture of 25% ethanol and 75% low octane (RON 91) gasoline, by volume (E25). Using maximum pressure as the point of knock onset reveals a research octane number in the engine of 111 for E25. This can be broken down into several components; the chemical octane number, the evaporative octane number, and the fuel sensitivity benefit of the engine.

Chemical octane number is the contribution due to the auto-ignition chemistry of the mixture. The gasoline component of this fuel has a research octane number of 90.8, which with an ethanol volume percentage of 25% leads to a chemical octane number of about 99.

Evaporative octane number is the contribution with direct fuel injection due to charge cooling through fuel evaporation. When injected into the cylinder, the fuel evaporates, cooling the in – cylinder mixture in the process, which lowers its tendency to auto-ignite. Estimates of this number for gasoline and ethanol are about 7 and 20, respectively. Since the fuel is 75% gasoline and 25% ethanol, this contribution was estimated as 10.

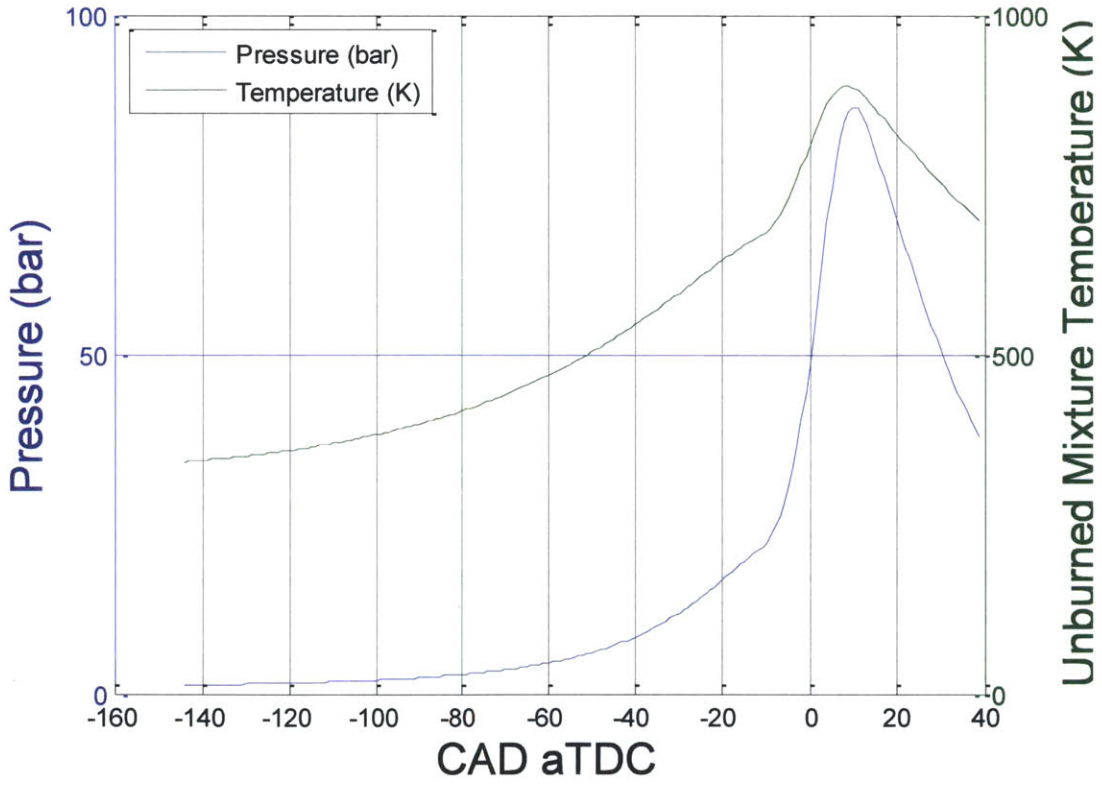

Figure 19: In Cylinder Unburned mixture temperature and pressure for an E25 knocking case.

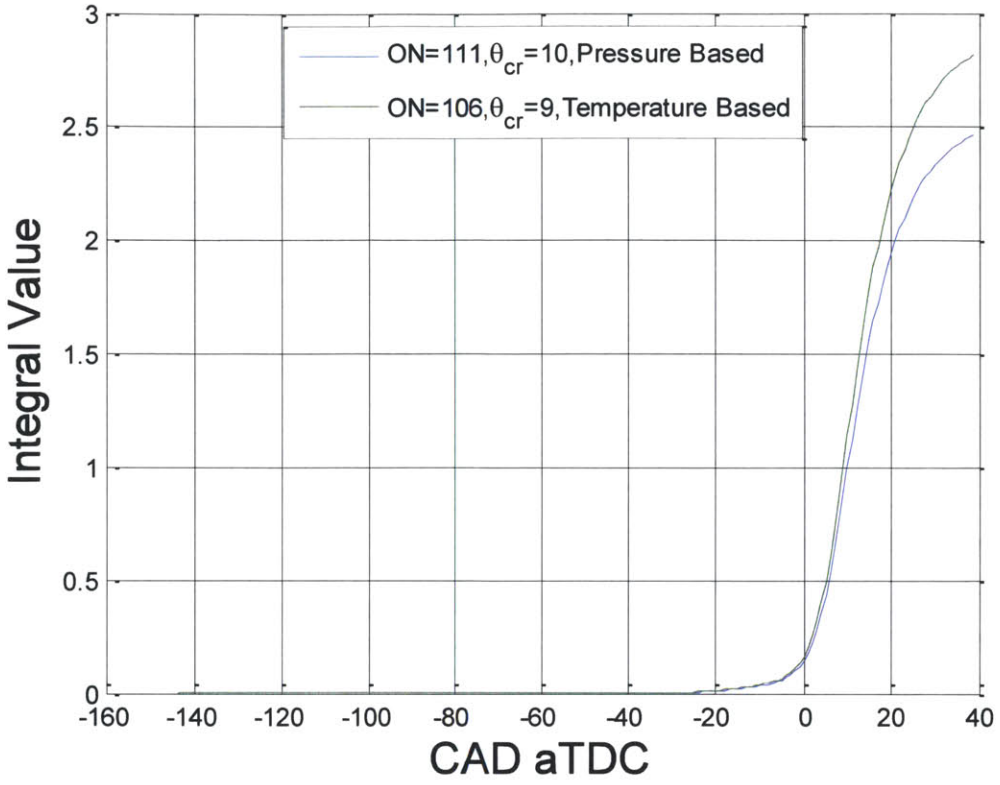

Figure 20: Knock Integral Evaluation for an E25 knocking case.

Table 2: Similar approach to table 1 done using E25

Maximum Pressure		**Maximum Temperature**	
Crank angle ATDC (deg)	Octane Number	Crank angle ATDC (deg)	Octane Number
10	**111**	9	106

Additionally, the sensitivity benefit is the increase in octane number due to differences between the current engine and the standard octane test engine. This contribution amounts to about two octane numbers, which in this case lead to a total octane number for E25 of:

99+10+2=111

This is close to the octane number (111) above, calculated using the auto-ignition time integral, again showing the approach works in calculating the octane number of new fuels.

The integral was evaluated over an interval beginning at 144 crank angle degrees before top dead center. This point represents the closing of the intake valve, when compression begins in earnest. The results for different fuels are shown below. The numbers calculated using the data from the GT Power model of the engine, as can be seen here are in most cases higher than the

references. As mentioned before, this can be due to uncertainties in the charge cooling effect and the octane sensitivity. For fuels with ethanol in them, the possible variation in octane number due to evaporative cooling was included as well.

Table 3: Octane Numbers done for additional fuels. Uncertainties due to charge cooling are mentioned as well.

	Experimental Octane Number	Chemical Octane Number [3]	Variations due to Evaporative Octane Number (if appropriate)
UTG91	91	90.5	-
UTG96	97	96.4	-
E10	100	95.05	8.3
E20	105	98.84	9.6
E25	111	100.4	10

5. Additions to the Performance Map

GT Power was used to determine how much ethanol would be required to suppress knock at each point by using the knock integral approach at each speed tested. This was done by using a PID controller to force the value of the auto-ignition integral to reach one by adjusting the throttle and waste-gate accordingly. To generate an upper bound on the knock onset lines the bounds of the integral were set to intake valve closure and peak pressure. For each fuel tested a knock onset line was determined from GT Power and superimposed on the performance map.

5.1. Extrapolation of Burn Rates

Since the burn rate was set in GT Power as an input it was needed to extrapolate based on current data taken from experiments done inside the engine. Data were taken with E85 at the range of tested speeds, from 1500 RPM to 3000 RPM. Burn duration data, defined by the number of crank angle degrees between 10% of the fuel burned to 90% of the fuel burned were shown in Figure 21.

What can be seen here is that at low loads the burn duration in crank angle degrees decreases as load increases and increases as speed increases. The sudden change in the trend above 1.4 bar manifold air pressure is due to the fact that at higher loads the limitation of peak pressure leads to a change in the behavior of the engine. Spark retard, which is implemented at high loads to limit knock, leads to slower burn duration as a result of the lower pressures and temperatures in the cylinder during combustion.

In order to deal with non-MBT behavior combustion retard was used to separate the cycles operating within MBT from others. Combustion retard was found by taking the fifty percent burned fuel crank angle degree of each point and comparing it with the point corresponding to the highest load.

$$Combustion\ Retard = \theta_{MBT} - \theta_{case}$$

If MBT was reached there should be positive and negative values of combustion retard. Therefore, when extrapolating only those cases where this case is satisfied were considered.

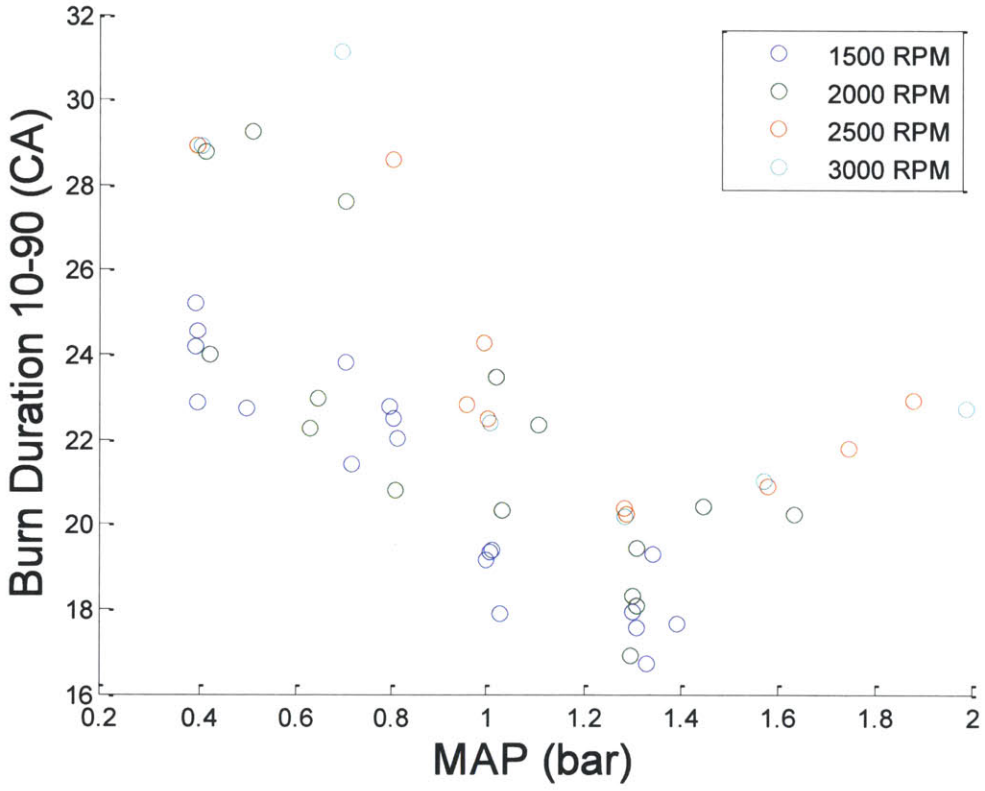

Figure 21: Burn Rate data used to extrapolate for GT Power simulations. Only data below 1.3 bars were used in the extrapolation function, since the 'kink' indicates a change in behavior.

5.2. MBT

Using GT Power performance maps of the engine were generated when operated at different compression ratios. They were shown as contour plots of efficiency superimposed on graphs of engine load, BMEP in bars v engine speed in RPM, as before, in Figures 22-24. The knock onset lines were added onto the performance maps for cases run with gasoline (UTG91), E10, E25 and E50.

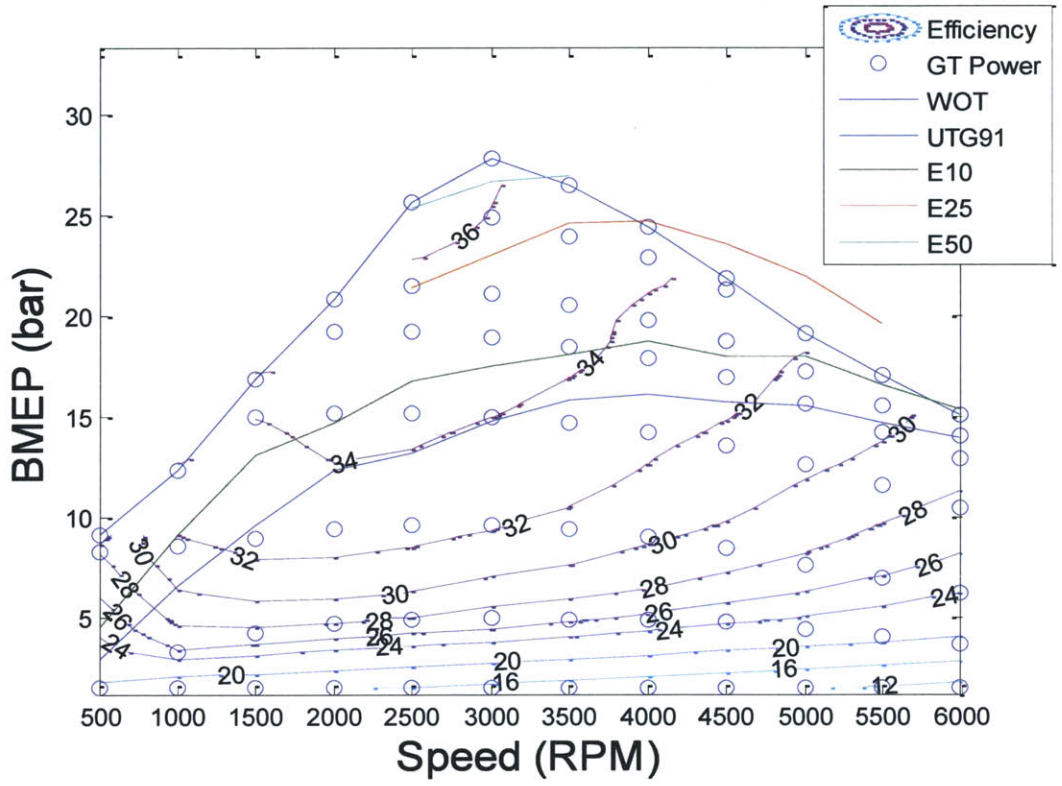

Figure 22: Performance Map for a compression ratio of 9.2

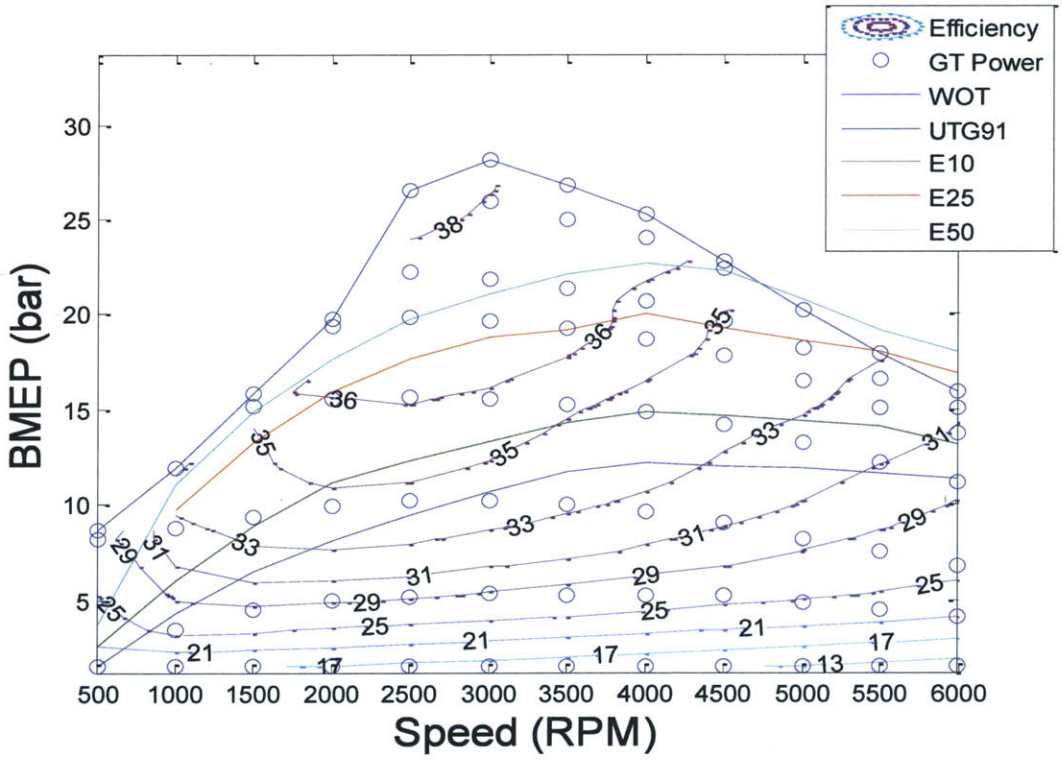

Figure 23: Performance Map for Compression Ratio of 11.5

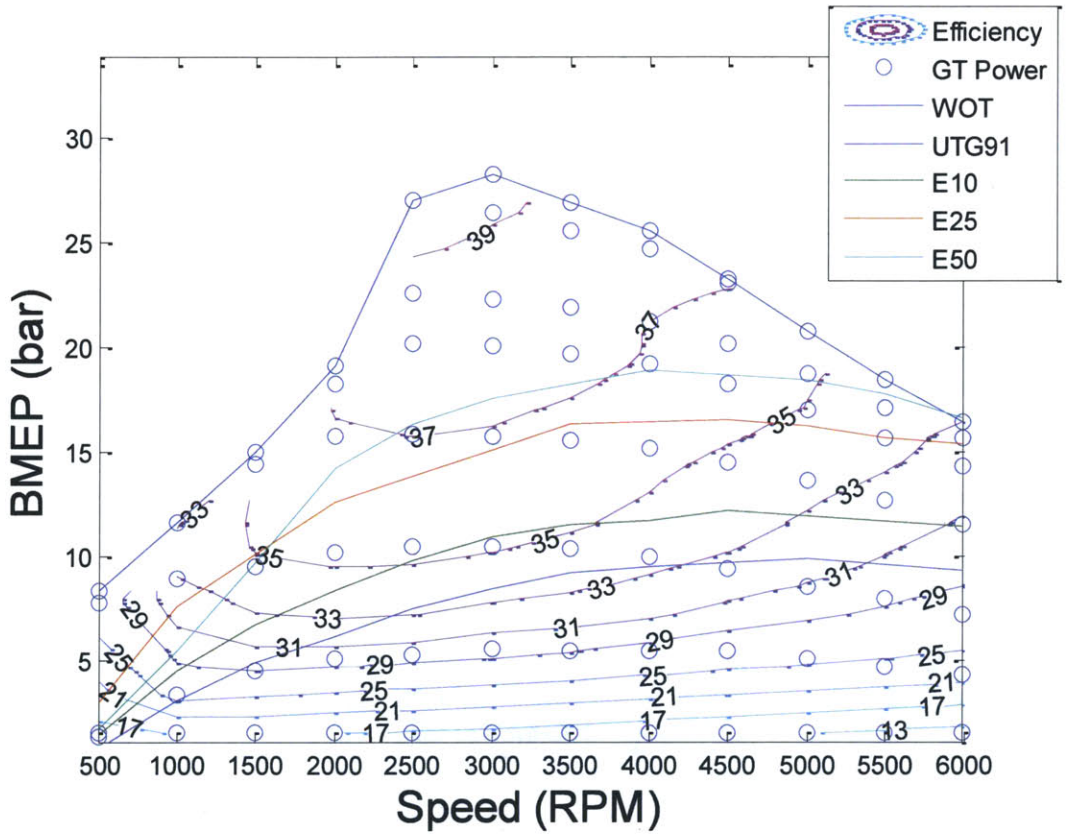

Figure 24: Performance Map for Compression Ratio of 13.5

Two conclusions can be reached upon looking at these data. First, efficiency increases when increasing compression ratio. Second, as compression ratio increases, the knocking threshold for each fuel decreases. Both trends are due to an increase in the pressure of the cylinder due to the higher compression in each cylinder. To illustrate this, peak pressure data for the three compression ratios is shown in Figure 25-28. For the compression ratio of 9.2 the peak pressure surpassed 100 bars at about 18 to 20 bar BMEP, which in the experimental E85 performance map was where efficiency began to level off. As compression ratio increases so does peak pressure for a given load, increasing the work done by the cycle and increasing its tendency to knock.

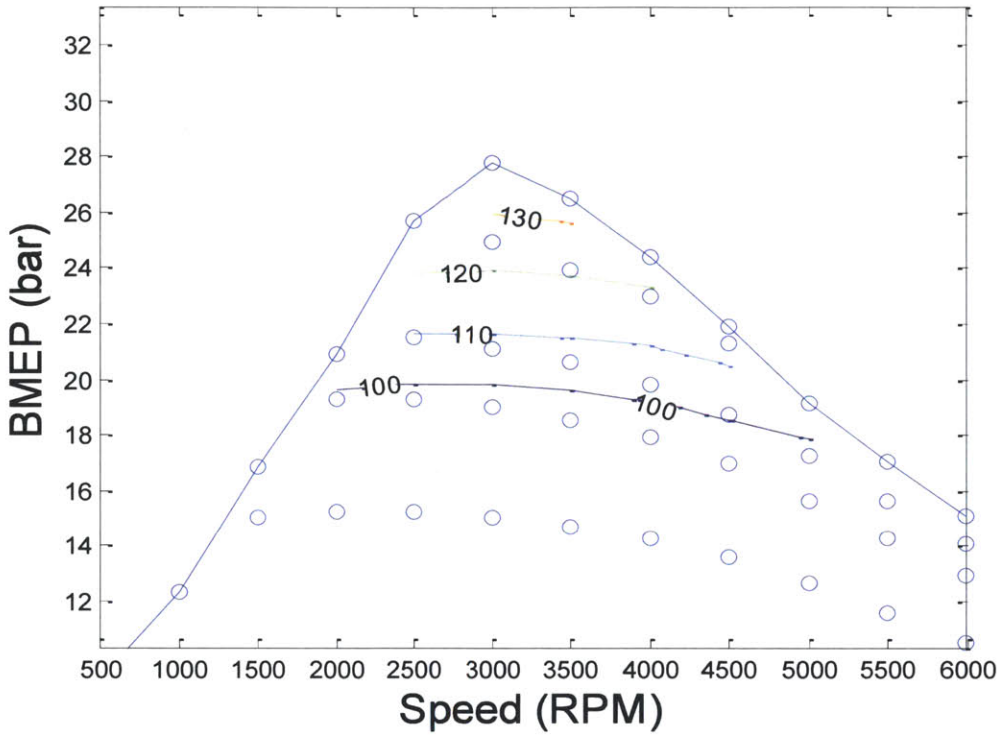

Figure 25: Performance Map with Peak Pressure Contours at CR=9.2

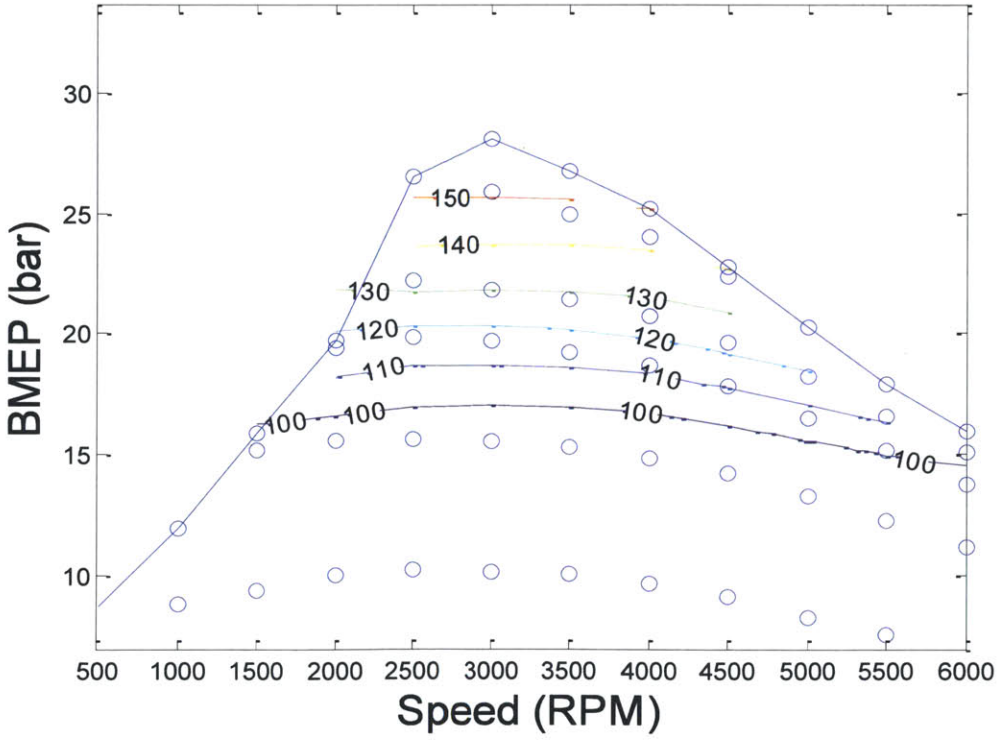

Figure 26: Performance Map with Peak Pressure Contours at CR=11.5

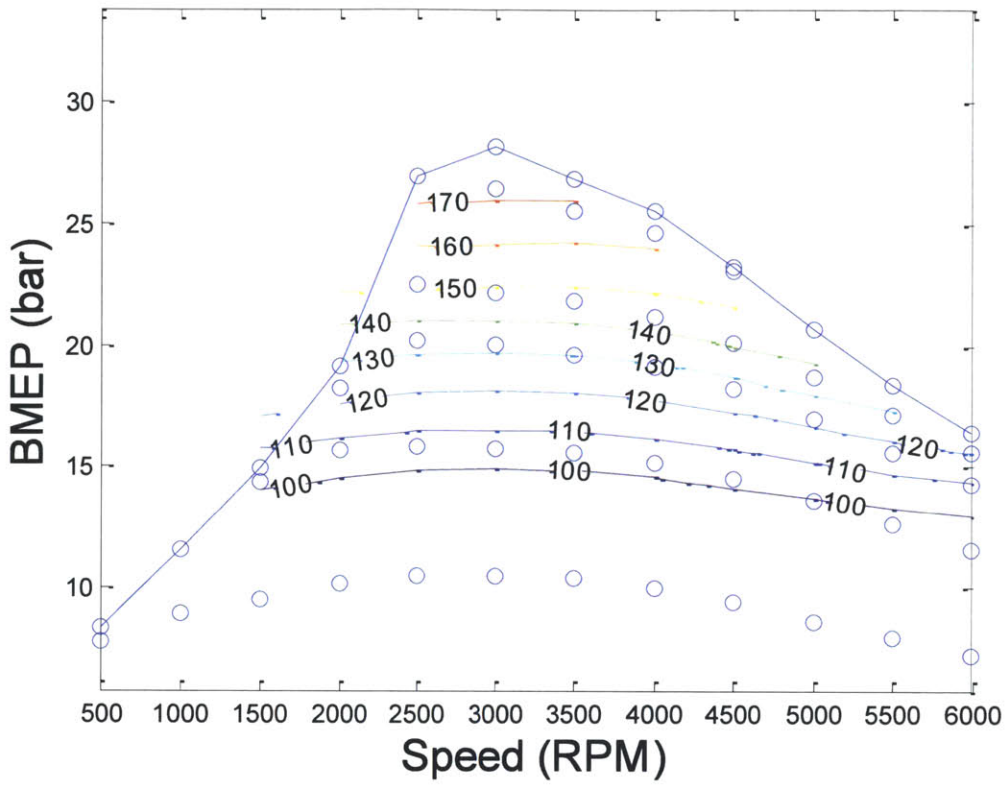

Figure 27: Performance Map with Peak Pressure contours at CR=13.5

5.3. With Spark Retard

To consider the effect of spark retard additional maps were generated using the following scheme. In regions where knock is not an issue the engine was run at MBT timing with UTG91. When the engine begins to knock with the base gasoline, the spark was retarded, up to a certain limit. The limits chosen here were 5 crank angle degrees after MBT timing and 10 crank angle degrees after MBT timing. Once that limit was reached, then ethanol was added to reduce knock while spark was still retarded at the limit.

Two trends can be seen when looking at these data in comparison with the data shown at MBT. First, the knock onset lines were higher. Second, the efficiencies are lower at high loads. The efficiency drops when retarding spark by 5 degrees and 10 degrees after MBT timing are on average 2.05 and 4.22 respectively. Both are due to the lower pressures and temperatures in retarded combustion. Lower pressures reduce the tendency of a fuel to knock, but they also decrease the efficiency of the fuel. This is because, for essentially the same inlet conditions, a lower pressure leads to less work, decreasing the efficiency.

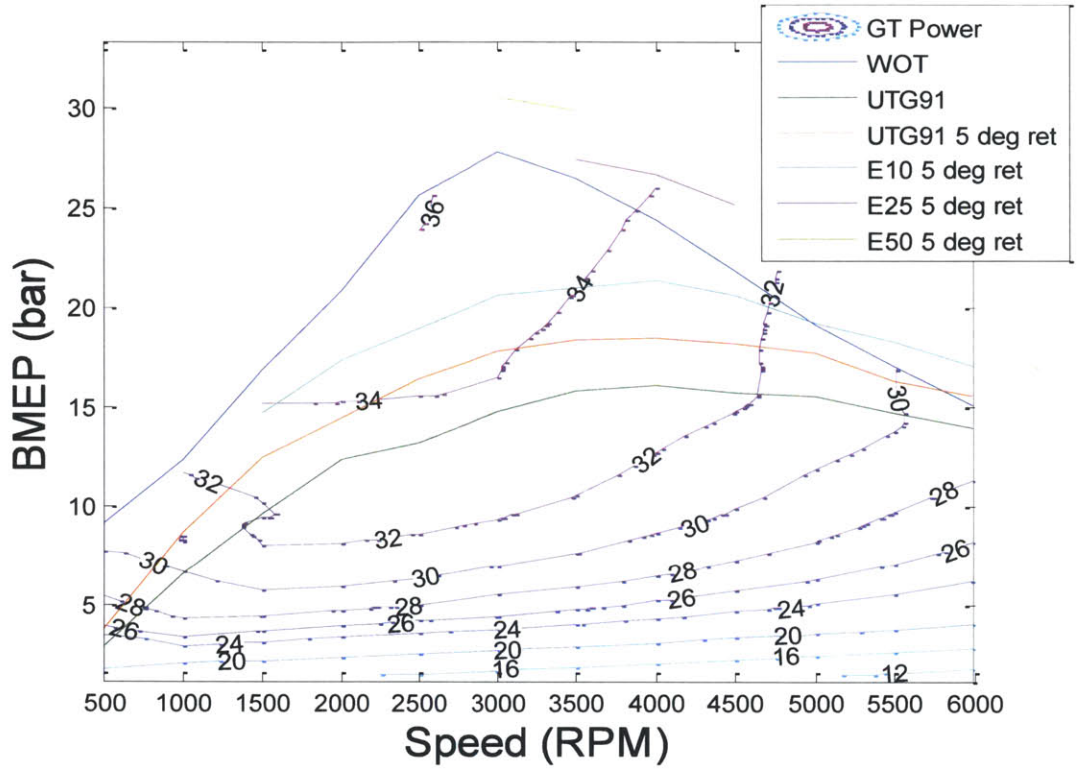

Figure 28: Performance Map with up to 5 degree retard at CR=9.2

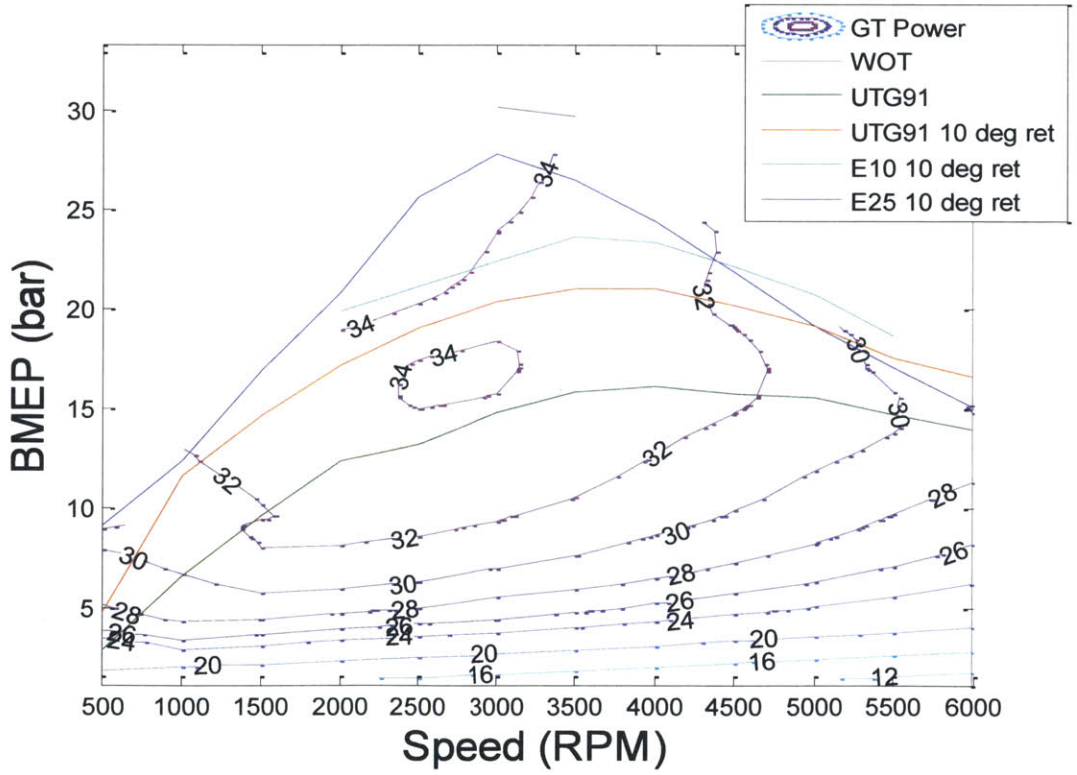

Figure 29: Performance Map with up to 10 degree retard at CR=9.2

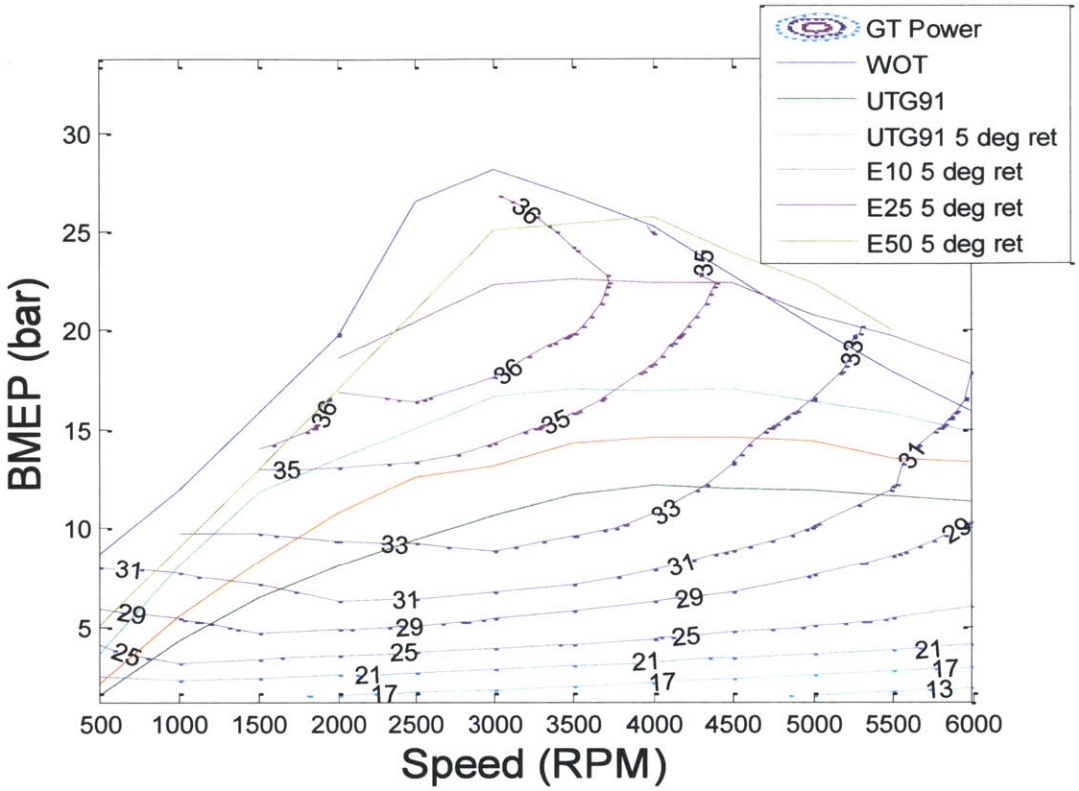

Figure 30: Performance Map with up to 5 degrees retard with CR=11.5

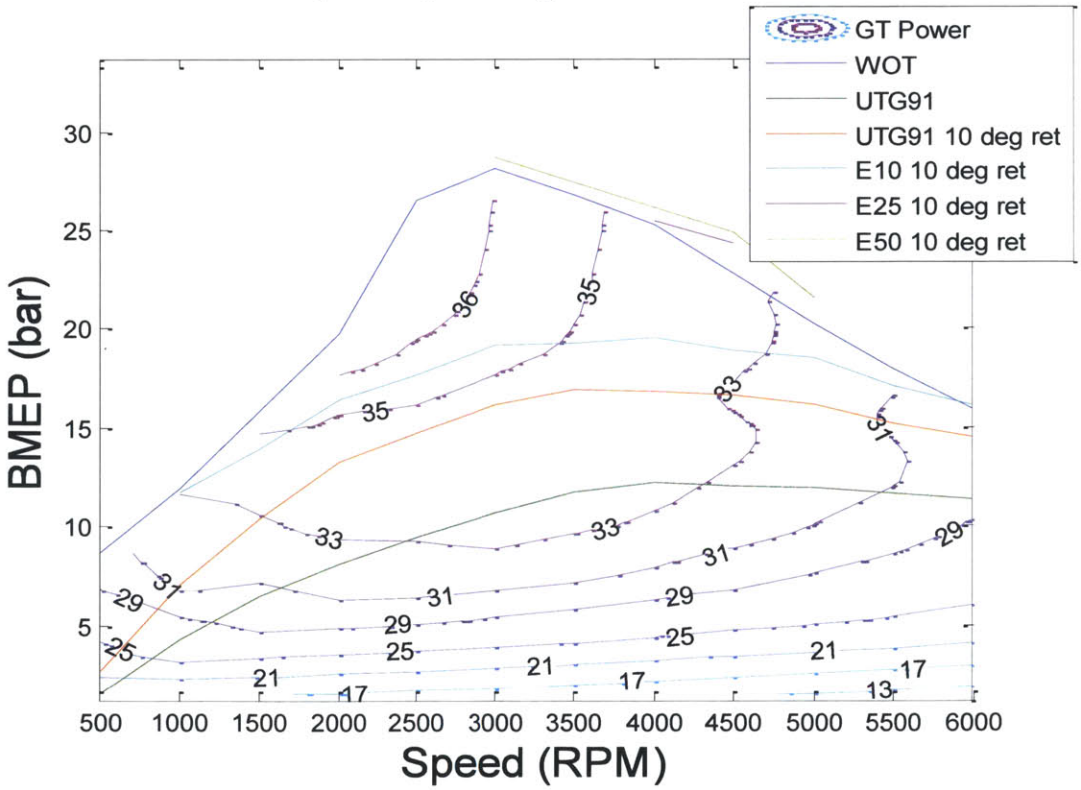

Figure 31: Performance Map with up to 10 degree retard at CR=11.5

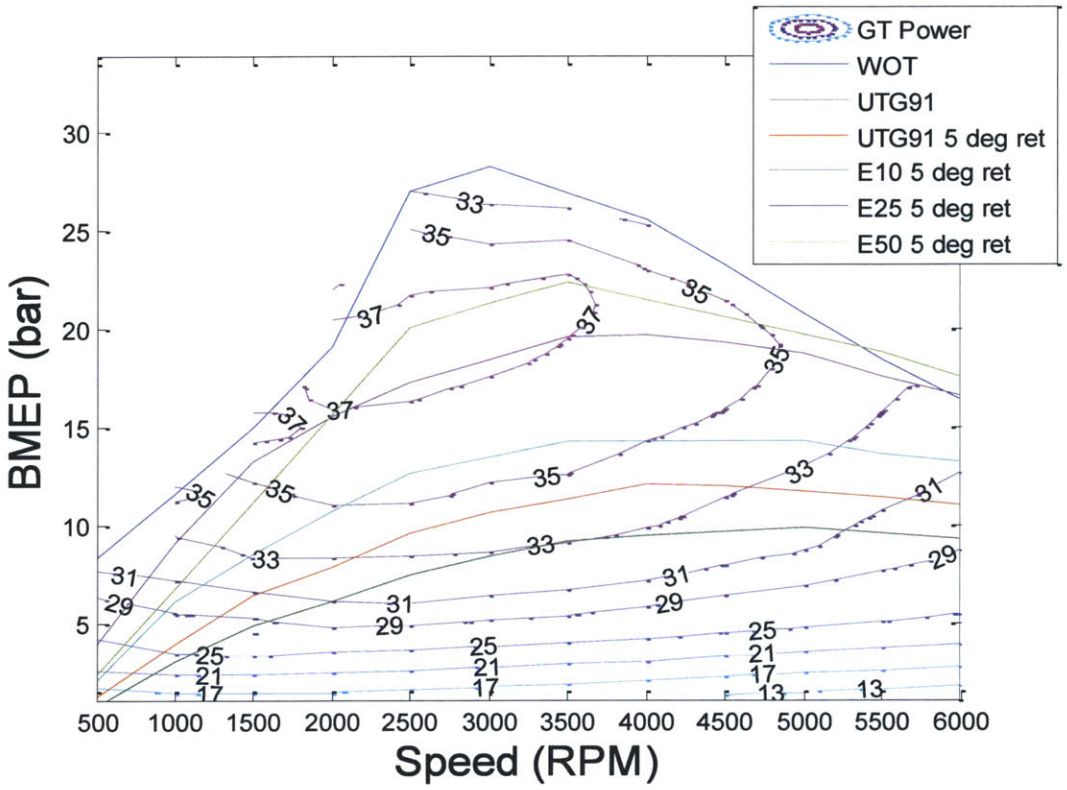

Figure 32: Performance Map with up to 5 degree retard done at CR=13.5

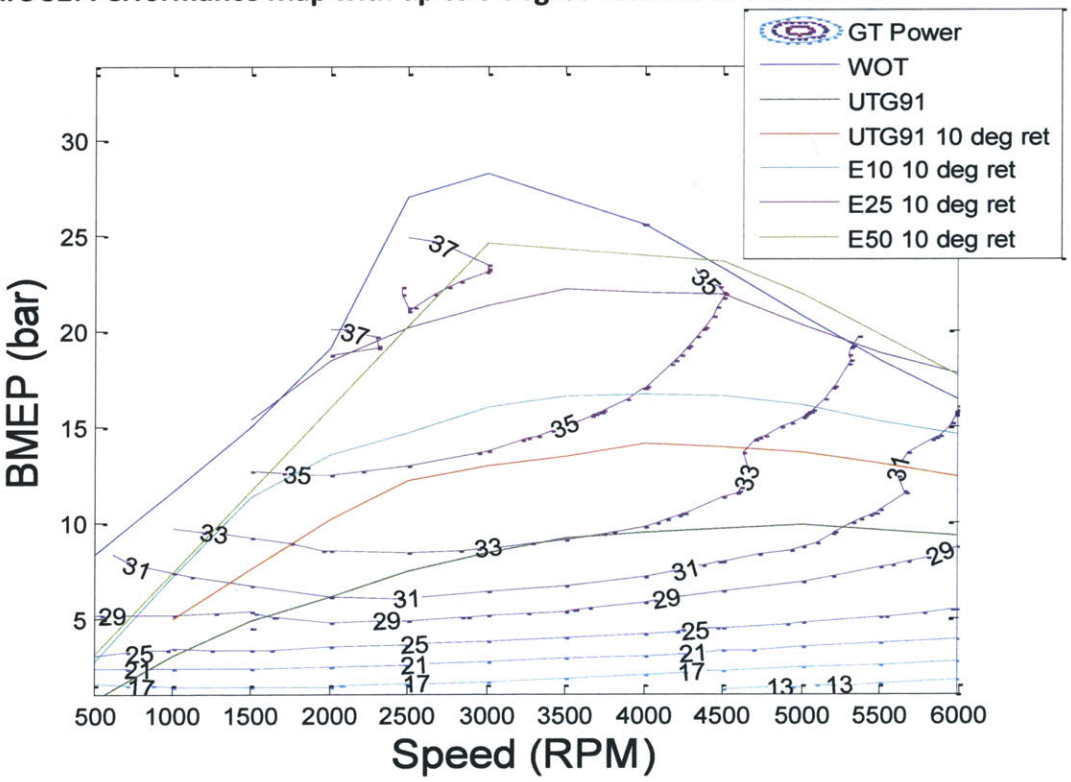

Figure 33: Performance Map with up to 10 degree retard at CR=13.5

6. Efficiency and Compression Ratio

Compression Ratio increased with efficiency and in order to validate the efficiency changes noticed in these performance maps the efficiency was compared to that of other cases previously studied. To compare compression ratios the efficiency was taken at the point corresponding to one quarter times the maximum torque at 1500 RPM. This point was chosen because for the majority of operation inside of a vehicle, the engine is near that operating point.

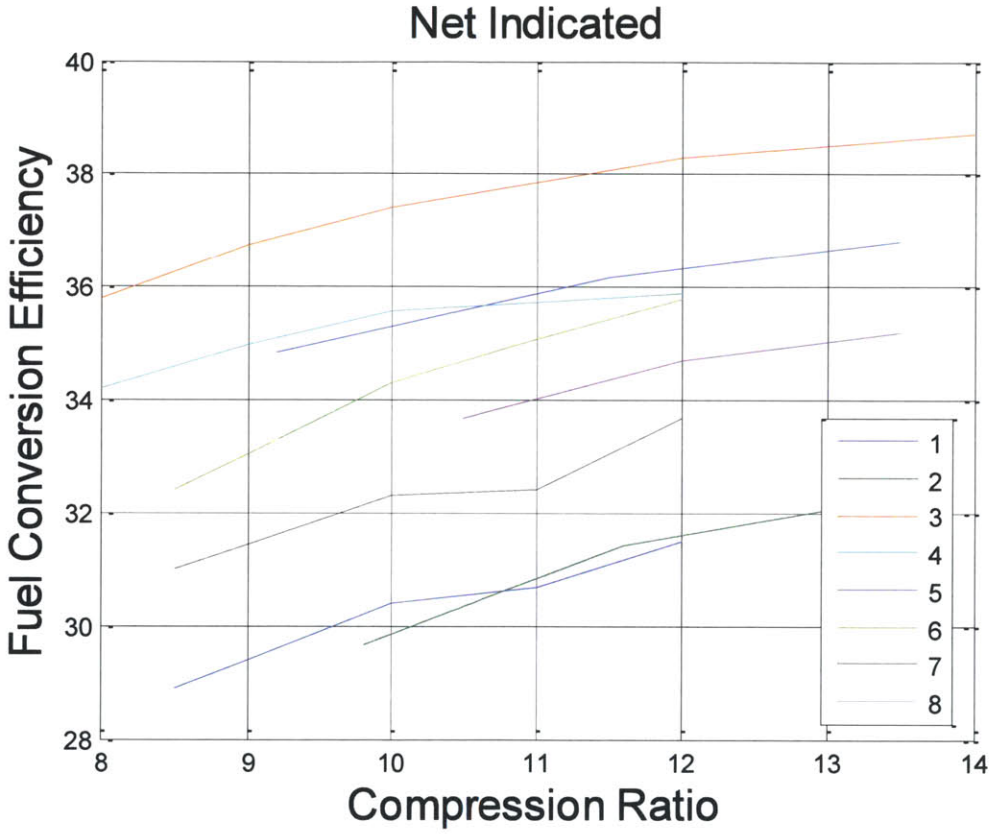

Figure 34: Indicated Fuel Conversion Efficiencies compared to other cases published in the literature

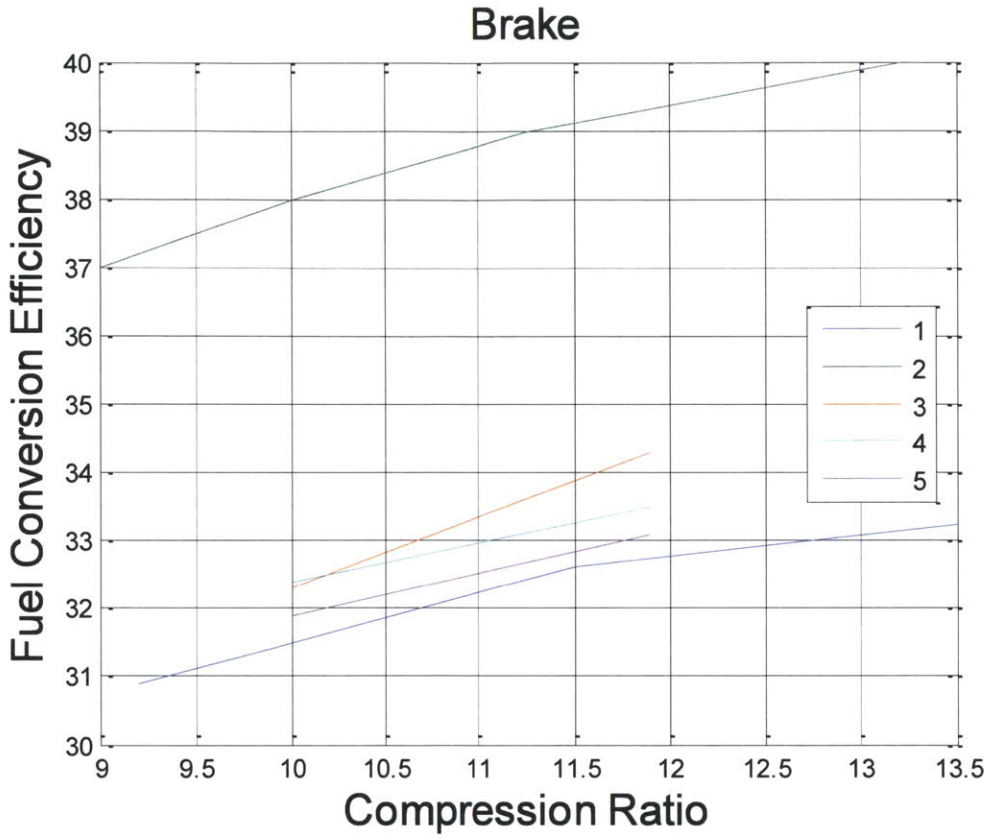

Figure 35: Brake Fuel Conversion Efficiencies compared to other data published in literature.

There was significant variation in the efficiencies shown because they were taken at different points in the operating map. Some were taken at part load, where efficiencies are lower and some are taken at wide open throttle, where efficiencies are higher. In order to generate a good comparison the data were normalized by the efficiency at a compression ratio of 10:1. This would normalize the changes in efficiency across different experimental runs. More information about the cases beings shown was provide in Table 4. When changing compression ratio from 9.2 to 13.5, the compression ratios in the current study, part load efficiency went from 30.9 to 33.2, a relative increase of about seven percent.

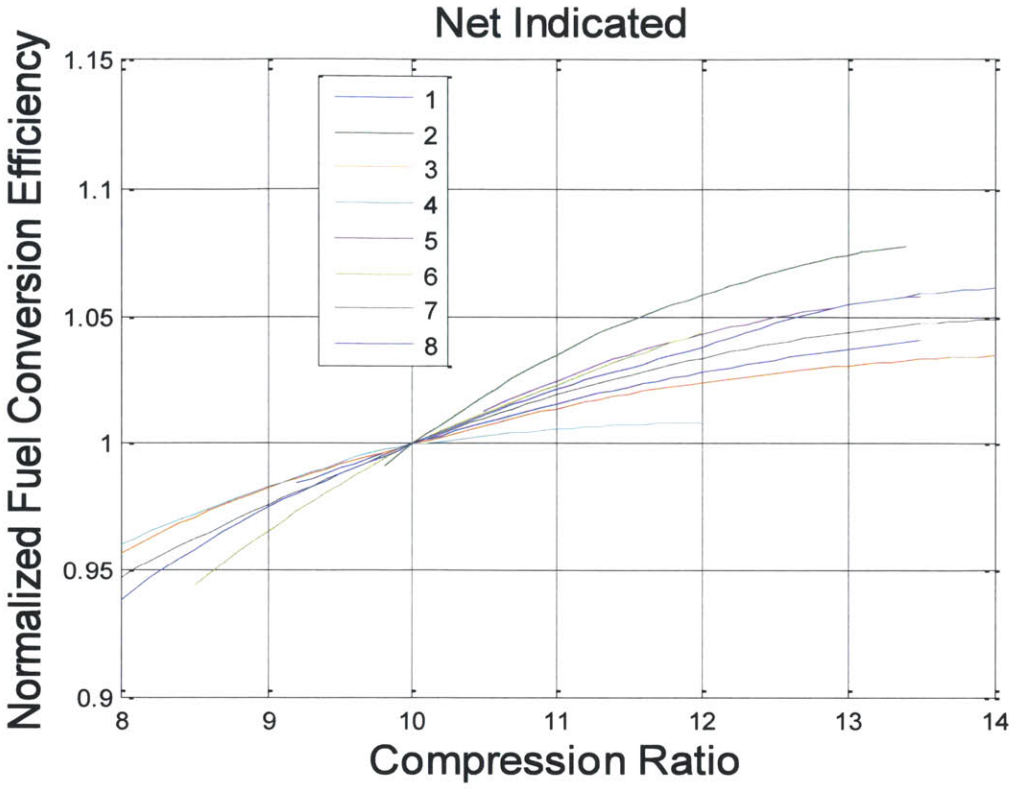

Figure 36: Normalized indicated fuel conversion efficiencies

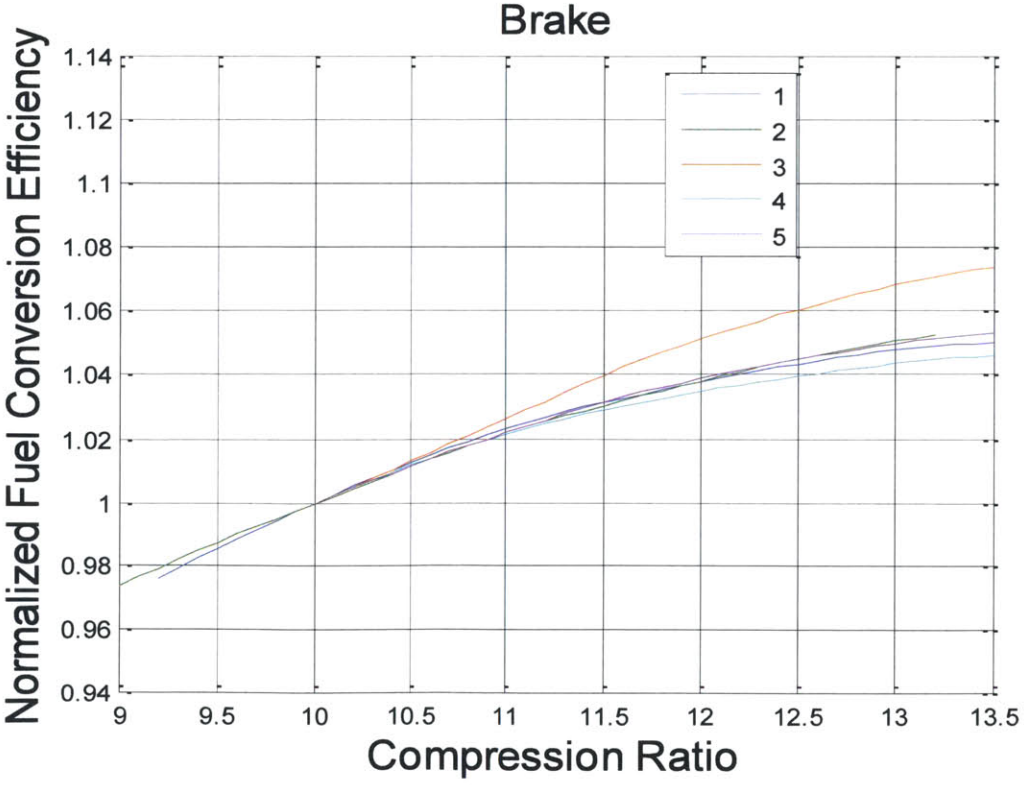

Figure 37: Normalized brake fuel conversion efficiencies

Table 4: Information and references of the efficiency v compression ratio data

Indicated Data		Brake Data	
Number in Graph	Information	**Number in Graph**	Information
1	1500 RPM 7 bar MAP	**1**	Part Load
2	WOT Efficiency Correlation [4]	**2**	1.2 bar MAP 3000 RPM [5]
3	500 cc engine [6]	**3**	1500 RPM, 5 bar BMEP [7]
4	250 cc engine [6]	**4**	2000 RPM, 5 bar BMEP [7]
5	6 bar IMEP, 2000 RPM [5]	**5**	2500 RPM, 5 bar BMEP [7]
6	1500 RPM 2.62 bar BMEP [8]		
7	2000 RPM 2 bar BMEP [8]		
8	1500 RPM 1 bar BMEP [8]		

7. Autonomie

To study how the engine would work inside of an actual vehicle, Autonomie was used to simulate the engine when running different drive cycles. Autonomie is a vehicle simulation program developed at Argonne National Laboratory. A map of fuel consumption as a function of engine speed and torque was fed into Autonomie and, using said map, Autonomie could simulate a vehicle when operating under different drive cycles. For every tenth of a second interval the torque, speed and fuel consumption of the engine were recorded. This was used to determine how the engine operates when placed inside an actual vehicle.

Three cycles were run in Autonomie: UDDS (meant to simulate city driving), HWFET (meant to simulate highway driving) and US06 (meant to simulate high speed, high acceleration and high variation in speed).

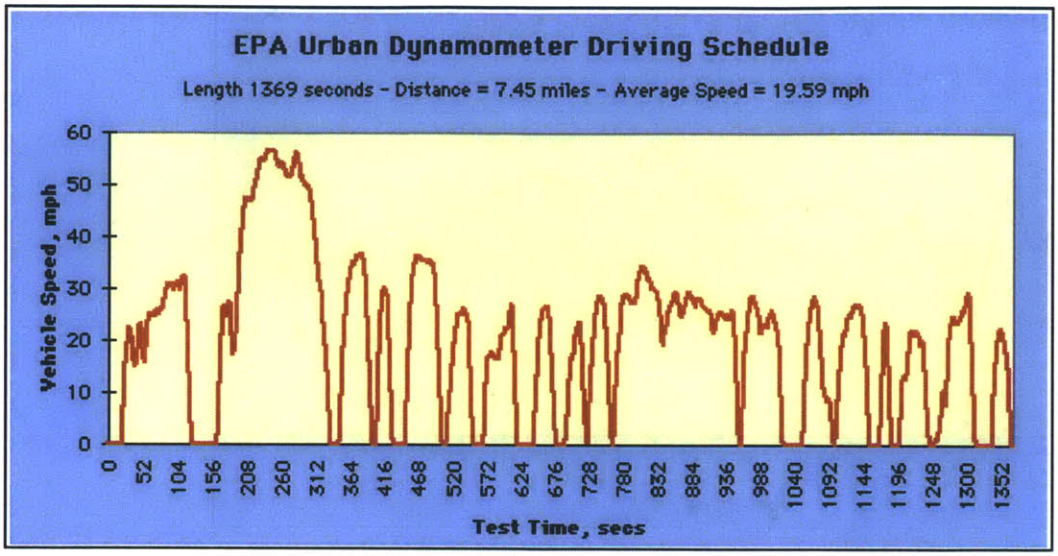

Figure 38: UDDS, meant to simulate highway driving [9]

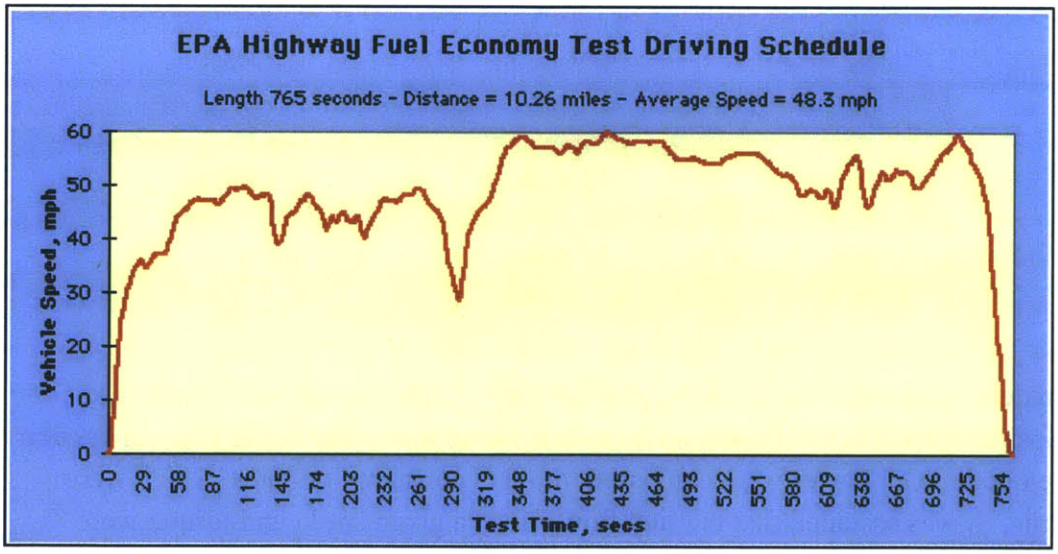

Figure 39: HWFET, meant to simulate city driving [9]

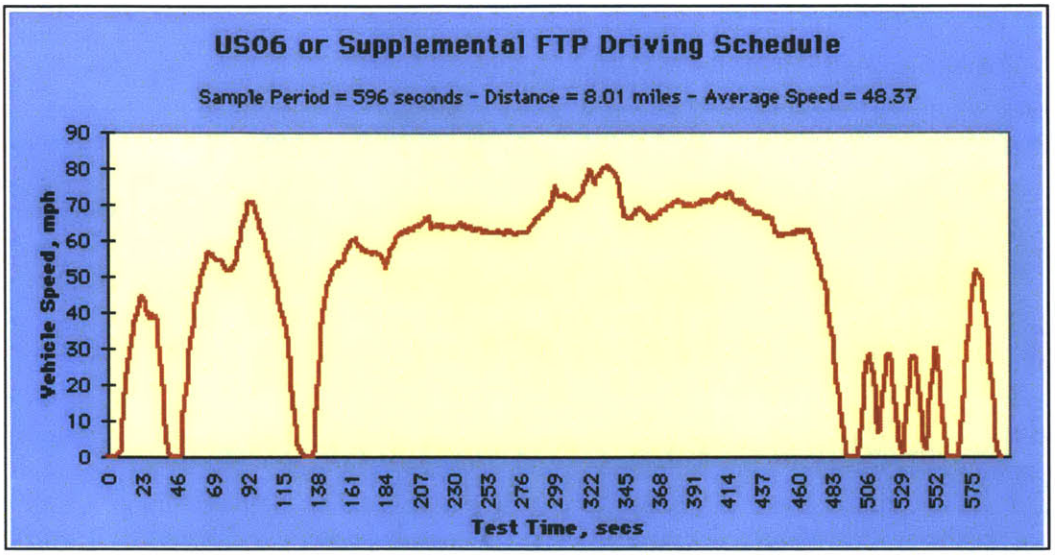

Figure 40: US06 additional cycle [9]

Table 5: More Information about the Drive Cycles [11]

	UDDS	HWFET	US06
Description	Urban/City	Free-Flow traffic on Highway	Aggressive Driving on Highway
Average Speed	20 mph	48 mph	48 mph
Time	31 minutes	12.5 minutes	10 minutes
Distance	17 miles	16 miles	13 miles
Max. Accel.	1.48 m/s^2	1.43 m/s^2	3.78 m/s^2

Since it has been determined that fuel conversion efficiency is independent of the fuel, the performance maps developed in GT Power were used in Autonomie. The brake fuel conversion efficiencies developed in GT Power were converted into fuel consumption rates, which were used in Autonomie. It was assumed that the fuel flow rate at a given speed and torque were expressed as follows:

$$f = \frac{N*T}{\eta*LHV}$$

Here f is the fuel flow rate in kg/s, N is the engine speed in rad/s, T is the engine torque in Nm, η is the brake fuel conversion efficiency and LHV is the lower heating value of the reference fuel in J/kg. Gasoline was chosen as the reference fuel. Using the efficiencies gathered from the performance maps fuel flow rate was calculated at each torque and speed point and used as an input to Autonomie. The output was defined as a gasoline equivalent, and by equating energy consumption those results could be used to calculate gasoline and ethanol consumption.

7.1. Base Vehicle

The vehicle chosen was a modified version of the conventional 2 wheel drive midsize sedan with automatic transmission, based on the Toyota Camry. For all simulations reported here the engine cylinder displacement was kept at 2.0L. Detailed information on the vehicle parameters is shown in the table below.

Table 6: Vehicle Parameters used in the simulation [11]

Component	Parameter	Value	Comments
Chassis	Chassis mas	990 kg	Vehicle Mass without power train
	Overall mass	1648 kg	Total Vehicle Mass
	Coefficient of Drag	0.3	
	Frontal Area	2.3229 m^2	
	Weight Distribution	64%	Fraction of weight supported by front axle
Engine	Max Torque (Nm)	[441.8, 446.5, 448.0]	Max Torque increased with compression ratio
	Displacement	2.0 L	Engine Displacement kept constant
Gear Box	Gear Ratios	[2.563, 1.552, 1.022,0.727,0.52]	5 speed gear ratio
Electrical Accessories	Power Losses	200 W	
Final Drive	Gear Ratio	4.438	Differential
Wheels	Wheel Radius	0.317 m	

7.2. Performance in the Driving Cycle

7.2.1. Fuel Economy

Using the data, three different metrics for fuel economy were developed. First, miles per gallon of gasoline equivalent could be determined from the unprocessed Autonomie results, shown in Table 7. This would serve as a proxy for the amount of fuel energy used over the course of each driving cycle with each amount of allowable spark retard and at each compression ratio.

Table 7: Miles traveled per gallon of gasoline equivalent used.

	UDDS	HWFET	US06
9.2 – MBT	29.30	40.79	27.24
- up to 5 deg retard	29.37	40.76	27.13
- up to 10 deg retard	29.37	40.76	27.10
11.5 – MBT	30.10	41.95	28.33
- up to 5 deg retard	30.39	41.89	28.27
- up to 10 deg retard	30.51	41.91	28.15
13.5 – MBT	29.93	42.25	28.81
- up to 5 deg retard	30.42	41.56	28.60
- up to 10 deg retard	30.67	41.63	28.42

From the data it can be seen that mileage increases with compression ratio. For the UDDS cycle mileage increases from 29.3 to 29.93, a relative improvement of 2 percent. The HWFET cycle mileage increases from 40.79 to 42.25 a relative improvement of 3.6 percent. The US06 driving cycle leads to a relative increase of 5.7 percent; 28.81 to 27.24.

These increases were all lower than the 7 percent increase in brake fuel conversion efficiency seen earlier. One reason for this difference is that the part load efficiency was taken at one fourth times the maximum torque, a fixed point relative to the performance map. As the compression ratio increased so did the maximum torque. As a result the part load point increased as well. In the performance maps it can be seen that at low loads efficiency is highly dependent on load, so this has the effect of decreasing the efficiency.

The fuel consumption over the entire cycle was converted to amount of gasoline and ethanol usage. This was done in order to determine how much gasoline and how much ethanol would be required for each case studied here.

Determining the amount of ethanol required was done by extrapolating the data used to create the knock onset lines on the performance maps. As a result ethanol fraction could be expressed as a function of speed and torque for each operating point. Since efficiency is independent of the fuel it was assumed that the total fuel energy of the gasoline-ethanol blend is the same as the gasoline equivalent. The resultant relationship is shown below:

$$\dot{m}_{sim} * t * LHV_{ref} = V_g * \rho_G * LHV_{gasoline} + V_e * \rho_e * LHV_{ethanol}$$

Here $\dot{m}_{sim}$ is the mass flow rate of the reference fuel from the simulation, t is the length of the time-step, LHV denotes the lower heating value, V denotes the volume and ρ is the density. For Autonomie t is 0.1 seconds. The subscripts gasoline and ref both refer to the gasoline used to blend with ethanol, UTG91. The volume of ethanol and gasoline could be related to the ethanol volume fraction E_f as follows:

$$(V_e + V_g) * E_f = V_e$$

Combining these two equations leads to the expressions below:

$$V_g = \frac{\dot{m}_{sim} * t * LHV_{gasoline}}{\rho_g * LHV_{gasoline} + \frac{E_f}{(1-E_f)} * \rho_e * LHV_{ethanol}}$$

$$V_e = \frac{E_f}{1-E_f} V_g$$

Using these equations the volume of gasoline and ethanol could be determined at each point in every cycle. Properties of the fuels relevant to these calculations are shown in Table 7.

Table 8: Fuel Properties Relevant to the Autonomie Based Calculations

	Density (kg/m^3)	Lower Heating Value (MJ/kg)
Gasoline (UTG91)	741.4	43.28
Ethanol	789	29.69

Mileage was expressed below as miles per gallon of gasoline and miles per gallon of ethanol. Two main results can be seen here. The first is that gasoline mileage can be higher than the effective mileage. The largest different here is at the US06 cycle at MBT timing at a compression ratio of 13.5. Here the miles per gallon of gasoline equivalent is 28.81 and the miles per gallon of gasoline is 33.86; a relative increase of 17.5%. This is because the addition of ethanol decreases the amount of gasoline required to provide the same energy; some of it was provided by the ethanol.

Table 9: Miles traveled per gallon of gasoline consumed.

	UDDS	HWFET	US06
9.2 – MBT	29.30	40.79	27.83
- up to 5 deg retard	29.36	40.76	27.36
- up to 10 deg retard	29.37	40.76	27.18
11.5 – MBT	30.24	42.14	30.43
- up to 5 deg retard	30.41	41.91	29.14
- up to 10 deg retard	30.51	41.91	28.57
13.5 – MBT	30.81	43.40	33.86
- up to 5 deg retard	30.75	41.84	30.46
- up to 10 deg retard	30.81	41.70	29.34

The estimates of miles traveled per gallon of ethanol consumed were shown in Table 10. The mileages shown here are significantly higher than that of gasoline. The lowest value of the entire simulation was 141 miles per gallon of ethanol with the US06 cycle at MBT and a compression ratio of 13.5. This is chiefly due to the fact that ethanol is only used where it is needed, when there is a risk of knock. Knock is only required at high load points, where the efficiency of the engine is higher than normal engine operation. For this reason the mileage estimates given for ethanol are much higher than with gasoline, in most cases by several orders of magnitude.

Table 10: Miles traveled per gallon of ethanol used.

	UDDS	HWFET	US06
9.2 – MBT	84409	$3.5*10^5$	932
- up to 5 deg retard	-	-	2337
- up to 10 deg retard	-	-	7156
11.5 – MBT	4829	6938	300
- up to 5 deg retard	$3.4*10^4$	63103	689
- up to 10 deg retard	$3.2*10^5$	$6.7*10^7$	1398
13.5 – MBT	769	1164	141
- up to 5 deg retard	2046	4575	341
- up to 10 deg retard	5002	19416	664

7.2.2. Ethanol Percentages

Using the data shown above it was possible to calculate the percent by volume of ethanol required under each driving cycle condition. Data were generated using the nine performance maps and the three drive cycles. The results are shown in Table 11.

Table 11: Ethanol Percentage done using the performance maps

	UDDS	HWFET	US06
9.2 – MBT	$3.47*10^{-2}$	$1.16*10^{-2}$	2.9
- up to 5 deg retard	0	0	1.16
- up to 10 deg retard	0	0	0.38
11.5 – MBT	0.62	0.6	9.2
- up to 5 deg retard	0.089	0.066	4.06
- up to 10 deg retard	0.0095	$6*10^{-5}$	2
13.5 – MBT	3.85	3.6	19.37
- up to 5 deg retard	1.48	0.91	8.21
- up to 10 deg retard	0.61	0.21	4.23

What can be seen here is that as the amount of allowable spark retard is increased the ethanol fraction decreased. Going from MBT to allowing up to 5 degrees of retard has the effect of reducing the amount of required ethanol by a factor of 2 to 6. This is due to the retarded combustion leading to lower pressures and temperatures in the cylinder, decreasing its tendency to knock. Also increasing compression ratio increases the amount of ethanol required by a factor of 2 to 5. This is due to the increase in pressure and temperature caused by the higher compression of the mixture.

7.2.3. Efficiency

In addition the average brake fuel conversion efficiency of each cycle could be determined by taking the total work done by the engine and dividing by the total energy input.

$$\eta = \frac{\int \tau\omega dt}{\int \dot{m} LHV dt}$$

Here η is the average brake fuel conversion efficiency, τ is the instantaneous engine torque, ω is the instantaneous engine speed, LHV is the lower heating value of the fuel, $\dot{m}$ is the mass flow rate and dt is the differential change in time.

Over the course of a driving cycle the engine can be used as a brake, when no fuel is fed into it. In this case, the torque becomes negative and the friction inside the engine is used to slow the vehicle down. This portion of the operation was not deemed relevant because no fuel is consumed during this process and the energy lost to friction in the engine was supplied by the fuel in the first place.

The results of removing the negative torque portion of engine operation were shown in Table 12. A key result seen here is that increasing the compression ratio tends to increase the efficiency. This is most pronounced in the US06 cycler, where at MBT the efficiency increases from 30.53 to 32.29. This leads to a relative increase of 5.5%. The smallest relative gain was about 2% for the UDDS cycle. Another result seen with the US06 cycle is the decrease in efficiency when spark retard in introduced. This is more pronounced with the US06 cycle because the US06 cycle includes higher loading points than the HWFET and UDDS cycle. As a result, the changes associated with spark retard have a stronger effect on it.

Table 12: Efficiency calculated only considering points where the torque is positive

	HWFET	UDDS	US06
9.2 – MBT	26.15	23.49	30.53
- up to 5 deg retard	26.13	23.54	30.41
- up to 10 deg retard	26.13	23.54	30.37
11.5 – MBT	26.88	24.13	31.76
- up to 5 deg retard	26.84	24.35	31.68
- up to 10 deg retard	26.85	24.44	31.54
13.5 – MBT	27.08	23.99	32.29
- up to 5 deg retard	26.63	24.37	32.05
- up to 10 deg retard	26.67	24.56	31.84

8. Comparison with Experimental Data

Estimated amounts of ethanol required for driving cycles were different for performance maps generated by experiments and simulation. To compare the differences, wide open throttle lines and knock onset lines of experiments and simulation were overlaid on the same graph. The first major difference noticed was the shape of wide open throttle line. The wide open throttle line of the simulation was higher than the experimental map since the data were limited by peak pressure remaining below 100 bars in the experiments. This limitation was not applied in the simulation. Also, they were different since the turbine behavior of the simulation was not exactly the same as the actual turbine. The maximum manifold air pressure using simulation was 2.4 bars while it was 2.0 bars for the actual engine.

One thing that was noticed when looking at the results was that the knock onset lines predicted by assuming knock occurs at peak pressure seem to be much more dependent on speed than the experimental data previously recorded. In theory knocking behavior should be dependent on speed because a lower speed would provide for more time during the combustion cycle for knock to occur.

Differences between the simulation and experimental results are shown in the Figure 41 below. Experimental results show knock onset to be much less dependent on load than what simulations suggest. One interesting results shown here is that between 1500 rpm and 2000 rpm, the simulation and experiment are in close agreement.

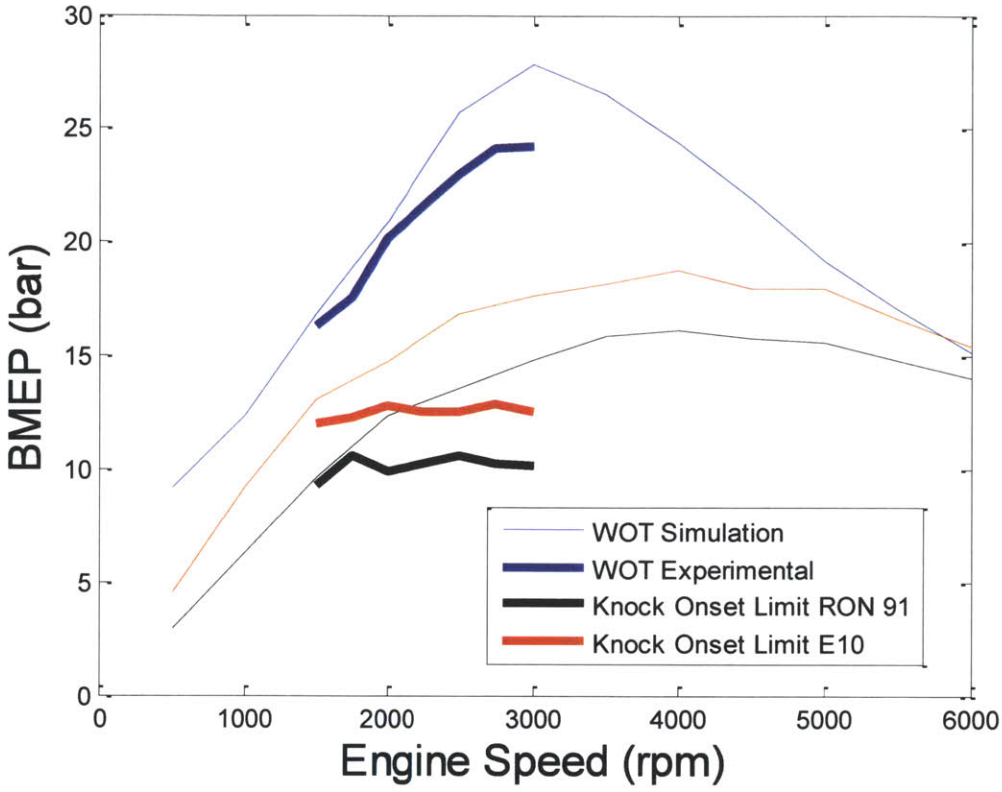

Figure 41: Comparison of simulation and experiment

One possible reason for the discrepancy was that experimentally knock onset can occur later than peak pressure. The simulations assume knock occurs at peak pressure. That provides an upper bound on knock onset lines for the majority of the map. In order to consider the possibility of varying knock onset and to provide a range of possible knock onset constraints, knock onset lines were generated for the same fuel (RON91) by widening the integration window used to predict knock. The results of extending the integration window by 5, 10, and 15 crank angle degrees are shown in the Figure 42 below.

Extending the integration window after peak pressure allowed more time for the end gases to knock. Using the Douad-Eyzat correlation this corresponds to a higher integral value for all cases being studied at the point define as knock onset. As the integral value becomes higher at each operating point, the load point at which the integral value reaches 1 decreases.

Another trend that can be seen here is that as the window is extended further, the change in load at knock onset decreases. The decrease in BMEP due to changing knock onset from peak pressure to 5 crank angle degrees after peak pressure is larger than the change due to an additional 5 crank angle degrees, almost by a factor of 2. This is because after peak pressure both the pressure and the temperature decrease. As the integration window is widened the decrease in BMEP becomes a diminishing trend.

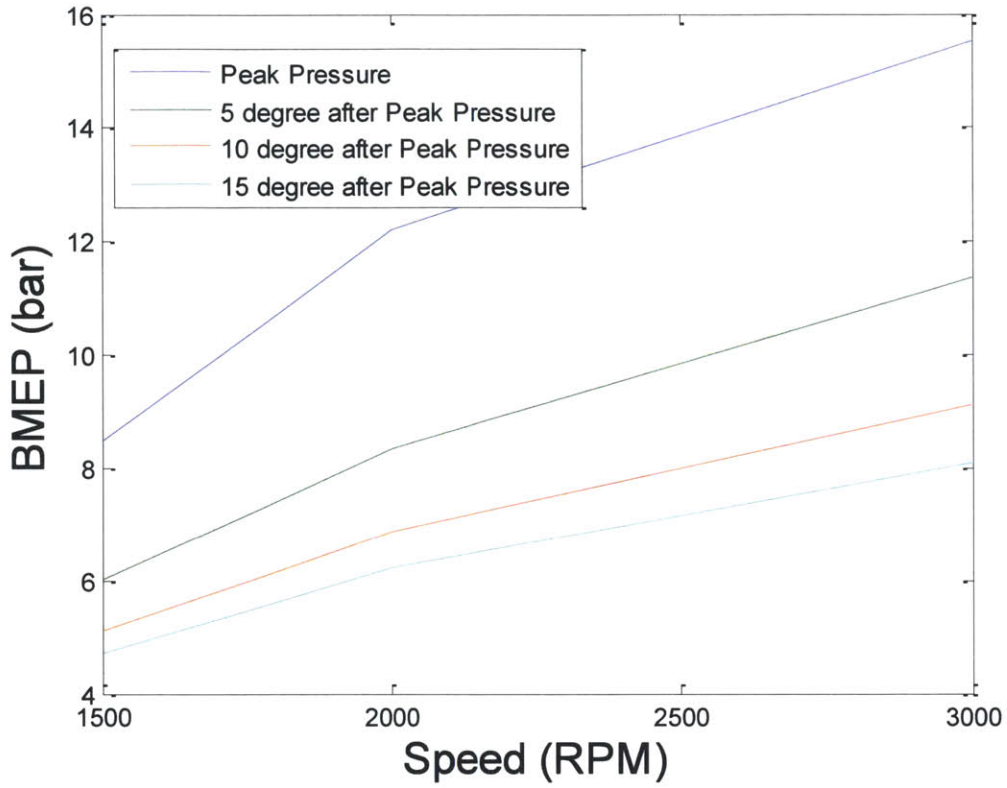

Figure 42: Here is the effect of changing the bounds of the auto-ignition integral to later than peak pressure. Blue represents setting knock onset to occur at peak pressure. Green, red and cyan are the results of setting knock onset to occur 5, 10 and 15 degrees after peak pressure, respectively.

8.1. Experimental Knock Onset at Different Speeds

In order to further explore the relationship between knock onset and speed data were taken at conditions where knock onset occurred and studied. Sample data is shown. An attempt was made to determine how peak pressure relates to knock onset by taking the filtered pressure trace, originally used to determine knock onset and the pressure profile that result from subtracting those results from the raw data. The shift in knock onset was determined by recording the passage of time, in tens of microseconds from peak pressure between the two traces. The results are shown for a set of example cases for UTG91 run at 1500 RPM, 2000 RPM, 2500 RPM and 3000 RPM. Each case is the worst knocking cycle at the spark timing and manifold air pressure tested.

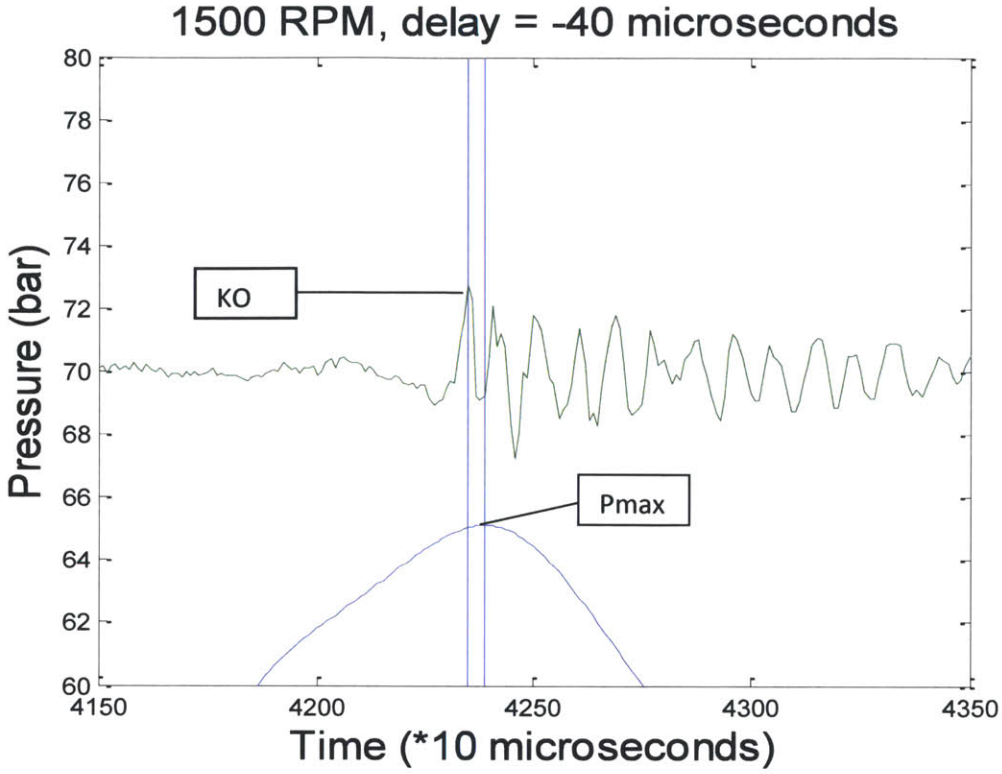

Figure 43: Sample Knocking Data at 1500 RPM, 10μs=0.09 CA

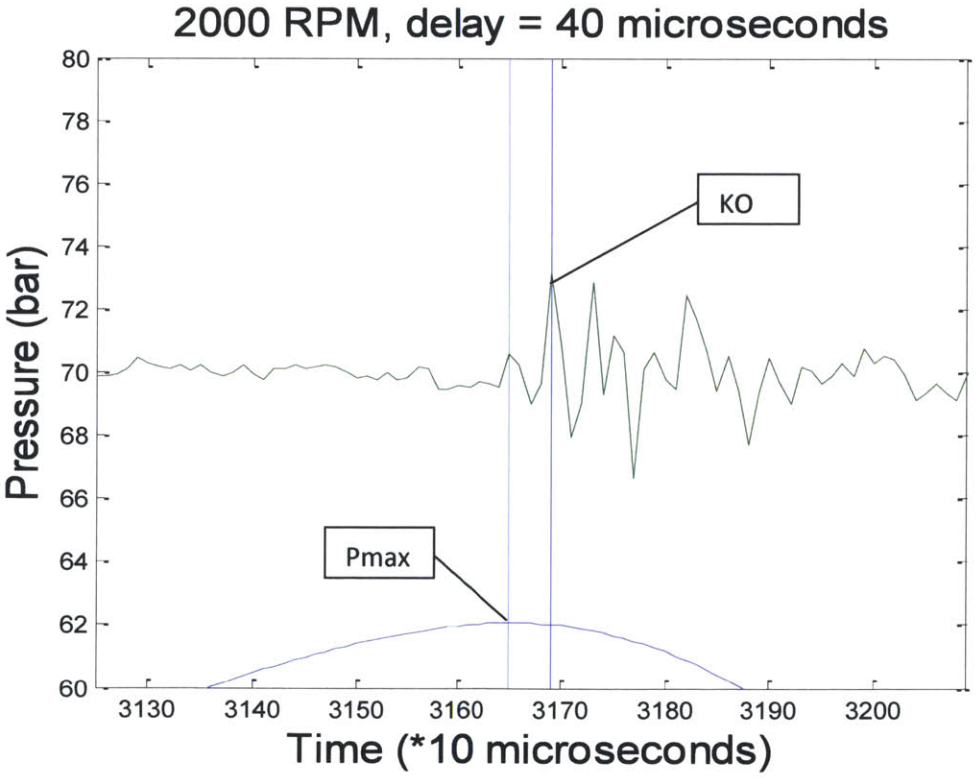

Figure 44: Sample Knocking Data at 2000 RPM, 10μs=0.12 CA

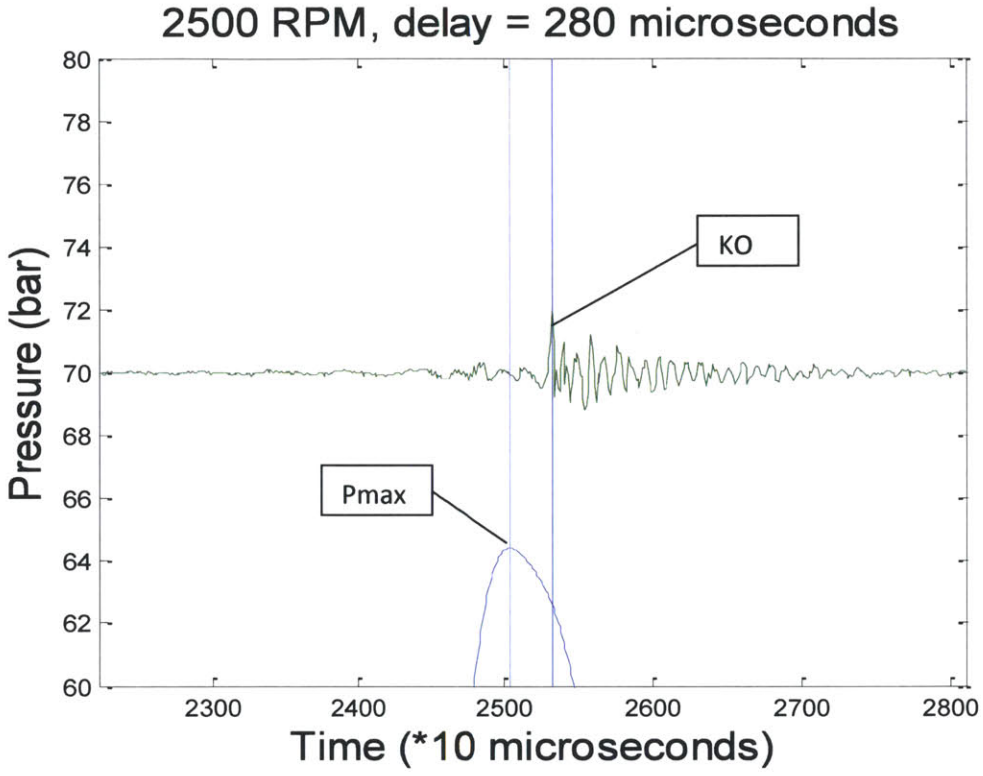

Figure 45: Sample Knocking Data at 2500 RPM, 10μs=0.15 CA

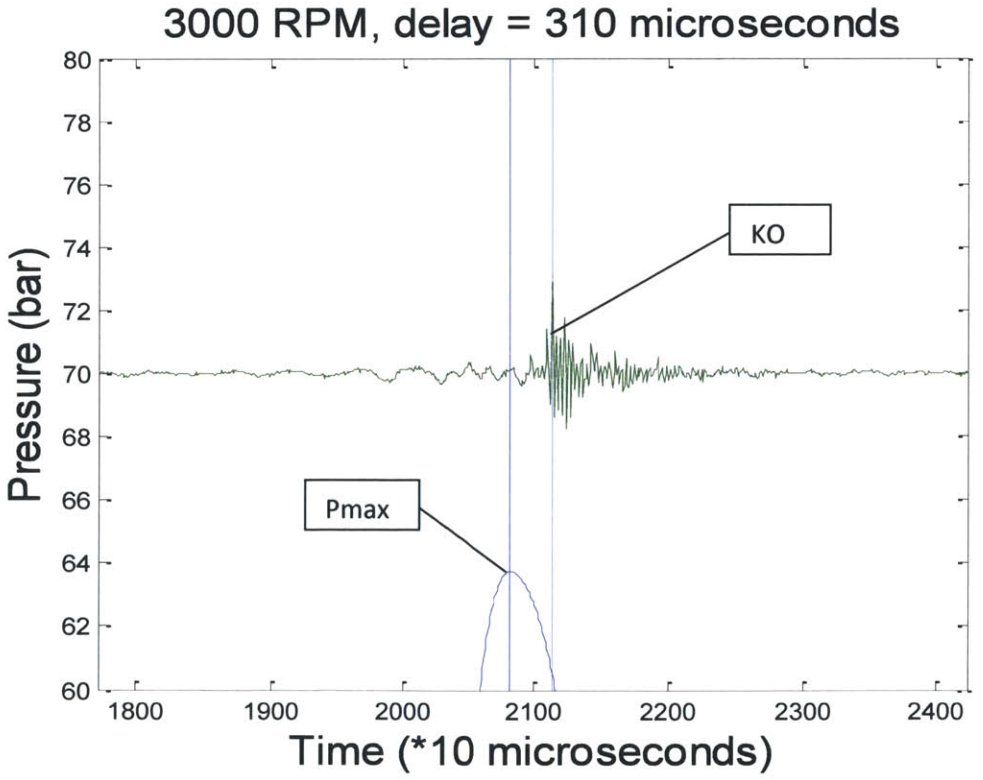

Figure 46: Sample Data at 3000 RPM, 10μs=0.18 CA

These results show that knock onset can sometimes occur several crank angles later than peak pressure. In order to get an average, data were analyzed by averaging over all knocking cycles. A simple linear curve fit of the data is shown in Figure 47.

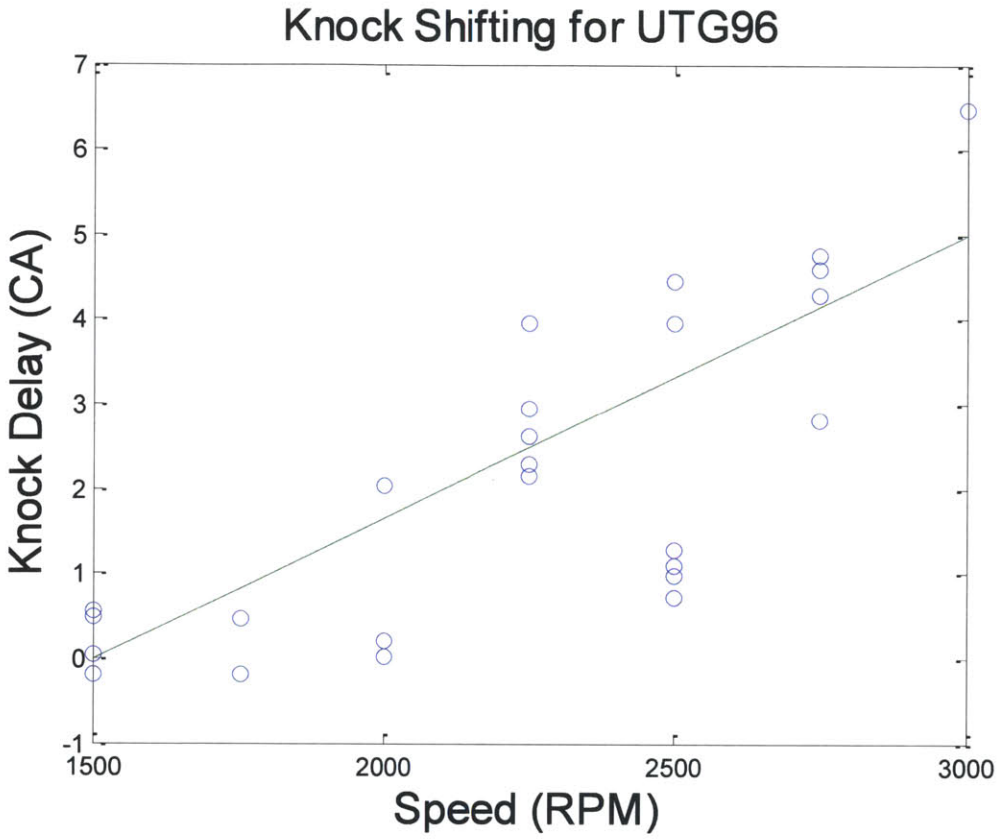

Figure 47: Knock data, delayed with an approximate linear curve fit. Each point represents the average over all knocking cycles at a fixed speed, load and spark timing.

Here is can be seen that it is possible to get a delay in auto-ignition of up to five crank angles after peak pressure. Previously it was shown that five crank angles was the range needed to keep the knock onset lines level, as in the experimental maps. The main result here is that the point at which knock onset occurs during combustion depends on speed.

9. Revised Results

It was deemed appropriate to consider an alternate case in which the knock onset lines were less dependent on speed, similar to the experimental results. In this new case the knock onset lines are level, meaning that the bmep where knock onset is set to occur for a given fuel was independent of the speed. In order to determine the relationship between load and ethanol fraction the bmep where knock onset was set to occur was recorded for a variety of gasoline-ethanol blends. Since comparison between simulation and experiment were fairly good in the 1500 RPM to 2000 RPM range, the loads corresponding to 1750 RPM were used.

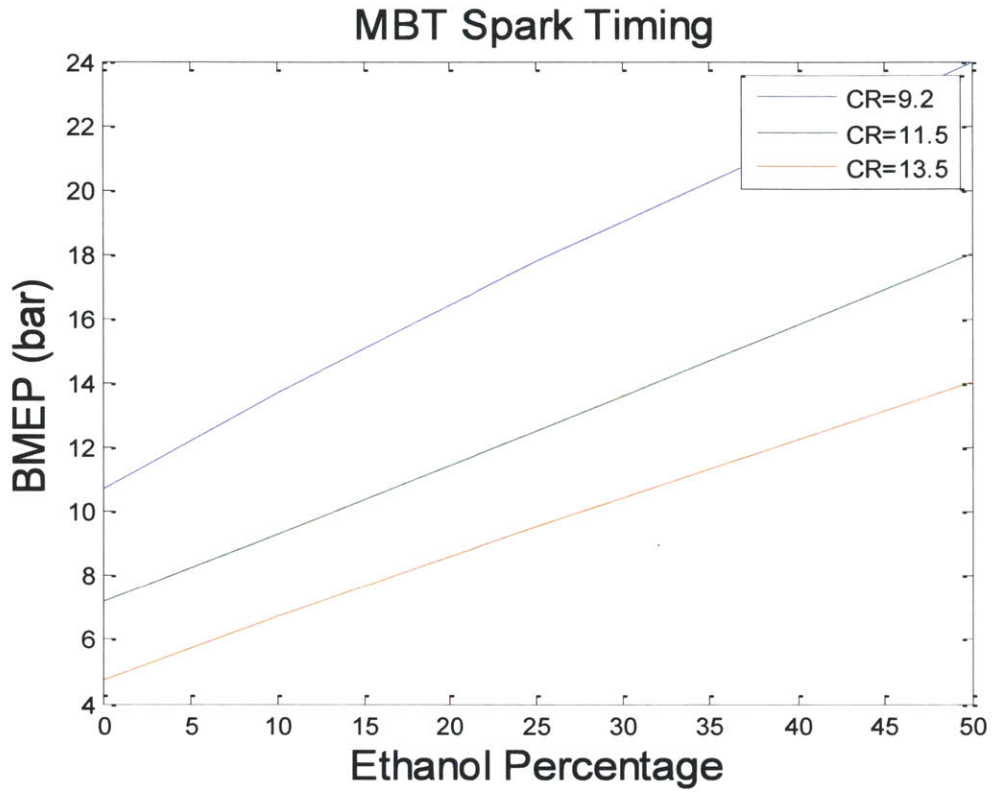

Figure 48: BMEP as a function of ethanol fraction at MBT

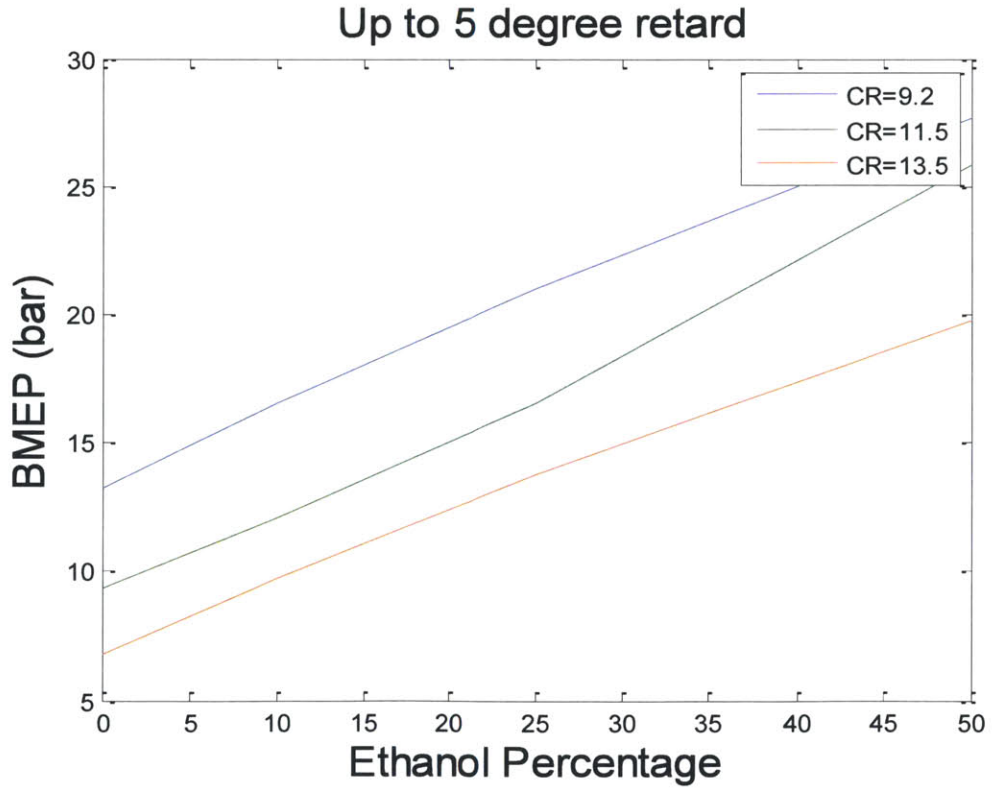

Figure 49: BMEP v. ethanol fraction with 5 degree retard

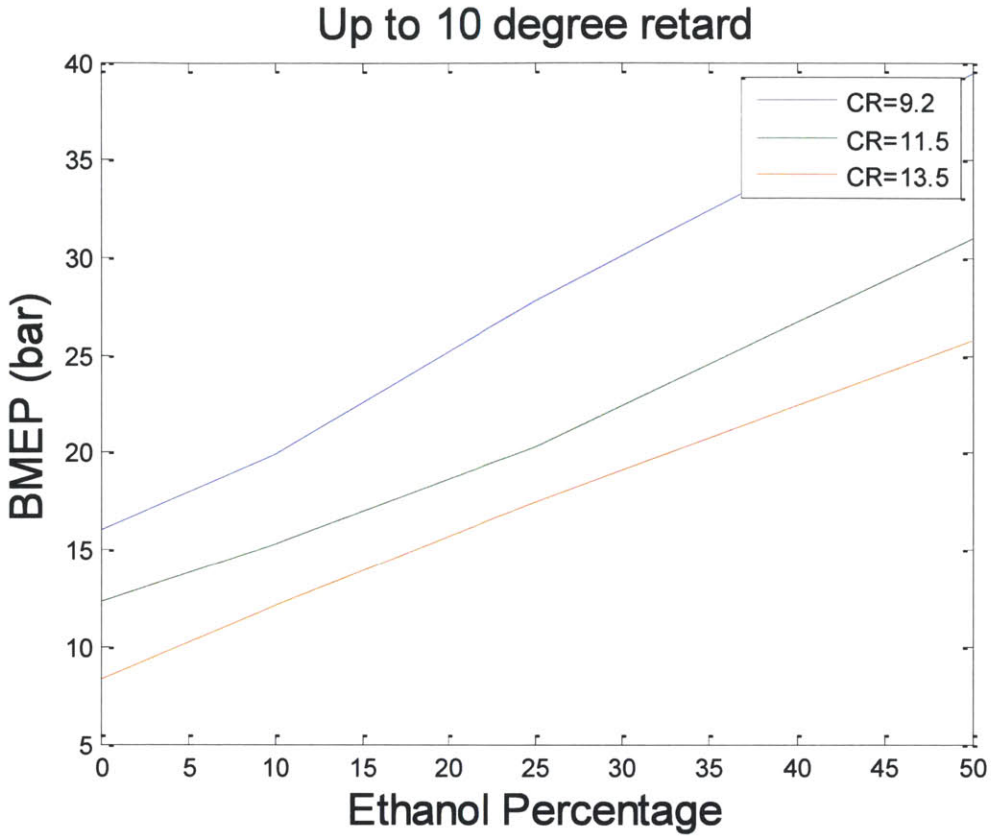

Figure 50: BMEP v. ethanol percentage at 10 degree retard

In the original performance maps the peak of the knock onset lines occurred at approximately 4000 RPM. As a result, for the majority of the performance map this new approach would lead to higher ethanol usage.

9.1. Ethanol Fraction

The generally expected trend is that with the new knock onset lines the required ethanol fraction will be higher because the revised knock onset lines are horizontal and, for a majority of the map, lower than the original map. This would require ethanol to be added at a lower point when previously it would have been fine to keep using gasoline. This is most clearly seen in the US06 cycle. Here, ethanol fraction is up to 10 percentage points higher with the new map in each case.

The trend is reversed when dealing with some of the cases with UDDS and HWFET. Some of the cases require lower ethanol percentages than the current model. This is also due to the fact that the knock onset lines are horizontal. At low speeds points require ethanol in the original map that did not in the new map, used with horizontal knock onset lines. As mentioned before, some points require ethanol in one case, but not in the other.

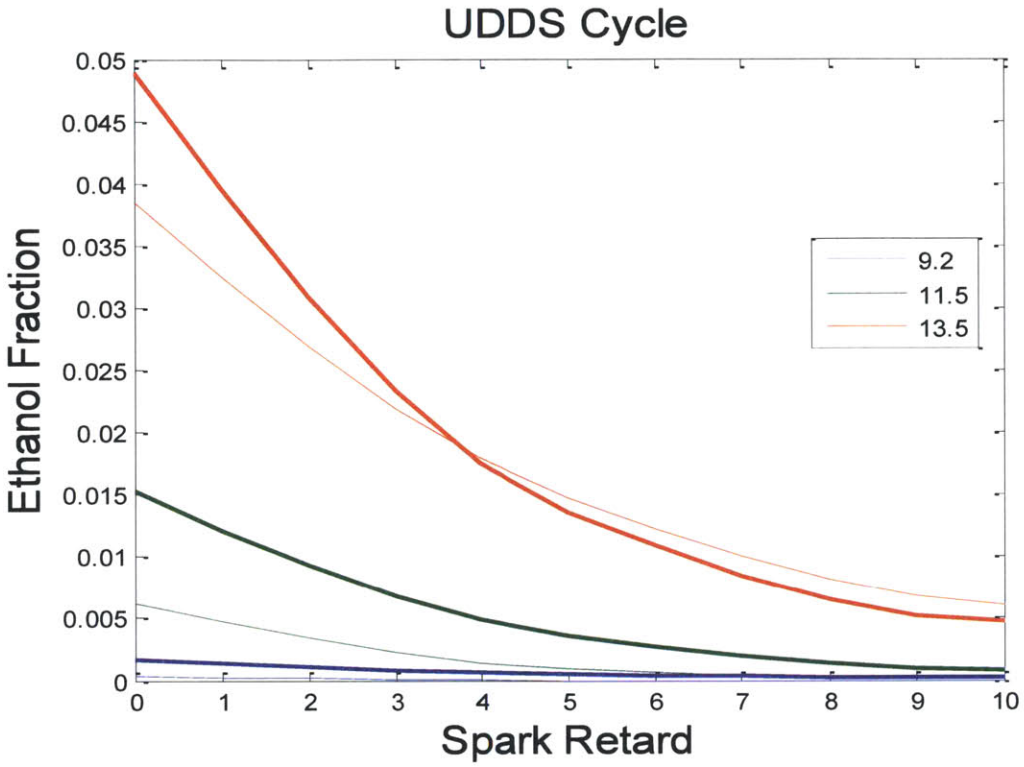

Figure 51: Comparison between original knock onset lines, (in bold) and new map with horizontal knock onset lines (thin lines). The key result here is that the original case, generally required more ethanol. This is due to the fact that the horizontal knock onset lines require fewer ethanol at low loads and speeds.

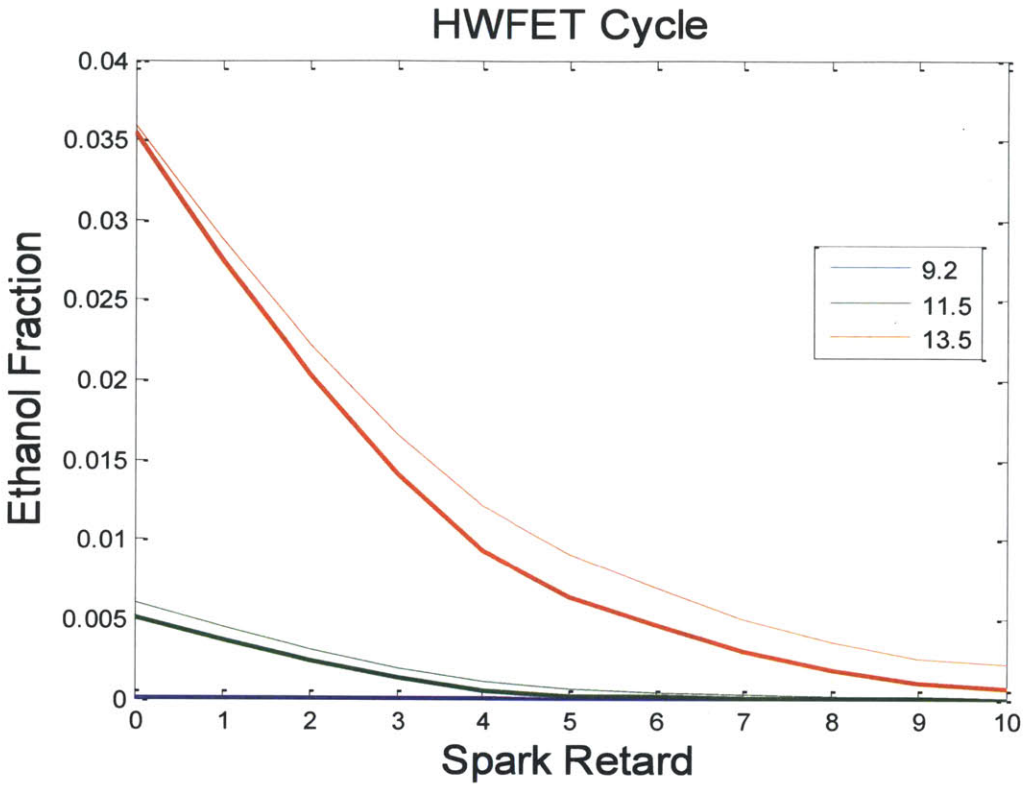

Figure 52: Ethanol fraction for HWFET comparing original (thin lines) with new knock onset constraints (bold lines)

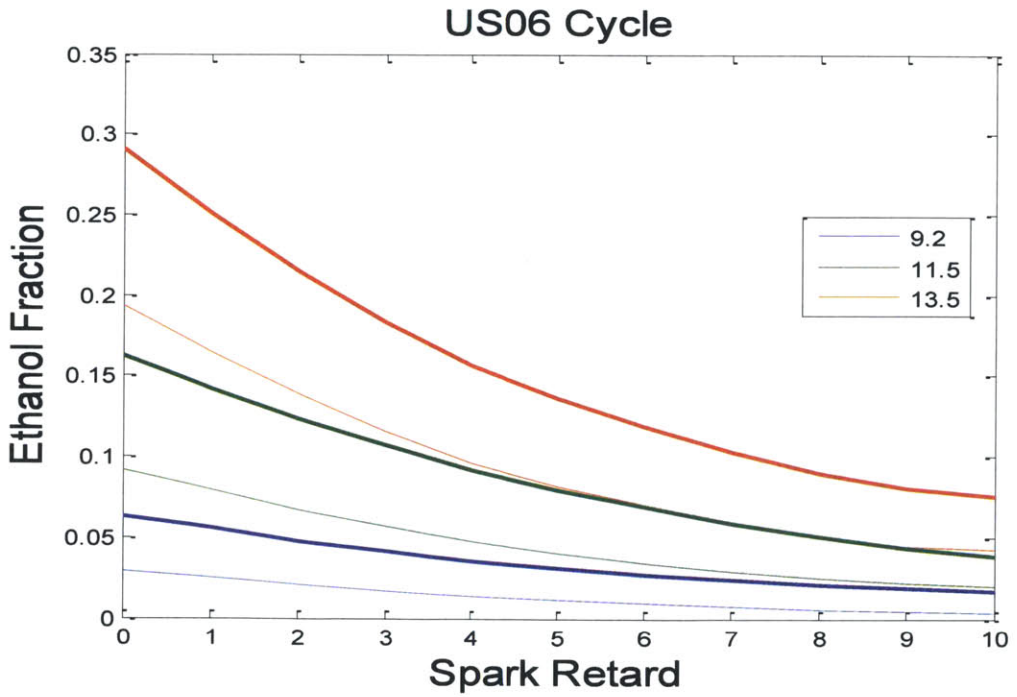

Figure 53: Ethanol fraction for US06 comparing original (thin lines) with new knock onset constraints (bold lines)

10. Findings and Conclusions

10.1. GT Power Modeling

GT Power was used to model experimental conditions in a turbocharged internal combustion engine at speeds operating between 1500 RPM and 3000 RPM. This was done by calculating the burn rate assuming poly-tropic expansion of burned species and poly-tropic compression of unburned species. Several simulation parameters were modified in order to make simulation agree with experiment. The best matches were found when combustion efficiency was set to approximately 95%, the heat transfer model was scaled by 1 to 1.1 and it was assumed that 30% of the available fuel – evaporation charge cooling was used to cool the walls and thus would not be available to cool the mixture.

10.2. Comparison of Different Fuels

It was determined that at low loads the energy conversion efficiency is essentially independent of the fuel used. At higher loads this is not the case because of limitations imposed by the type of fuel and engine, i.e. knocking or peak pressure in the cylinder. When comparing different fuels, the difference in efficiency was less than 1%. Therefore, it can be concluded that over the lower two – thirds of the performance map, the energy conversion efficiency of the fuel is independent of the fuel used.

10.3. Octane Number

GT Power was used to simulate experimental conditions in the cylinder. By matching the pressure profile in GT Power with the experimental pressure profile it was possible to calculate cylinder parameters that could not be measured in the current setup, such as mixture temperature. By using the temperature and pressure of the unburned mixture from the beginning of compression to knock onset, effective octane numbers could be generated. Octane numbers found ranged from 91 for UTG91 gasoline to 111 for E25. The numbers found for these fuels were, in some cases up to 10 octane numbers higher than those reported by other studies. These were attributed to differences, engine to engine, which results from fuel sensitivities (RON – MON). This amounts to two octane numbers. Another contributor to the difference is effect of charge evaporative cooling which, for the fuels tested can be as high as ten octane numbers.

10.4. Higher Compression Ratio

In GT Power several performance maps were created at different compression ratios, assuming that the fuels are interchangeable in the cylinder, other than knock constraints. This meant that it was possible to run the engine at MBT indefinitely and mitigate knock by adding modest amounts of ethanol within the cylinder. It was determined that an increase in compression ratio from 9.2 to 13.5 leads to a relative increase in brake fuel conversion efficiency of 7 percent at

typical part load conditions; 30.9 to 33.2. This is supported by comparison with previous studies of efficiency and compression ratio.

10.5. Spark Retard

In cases where it is desired to minimize the amount of ethanol, increasing spark retard is applied first up to 5 or 10 crank angles after MBT timing if knock is predicted. Ethanol is added afterwards once the maximum amount of spark retard is reached, depending of the severity of knock. This would shift the knock onset lines upward, requiring smaller amounts of ethanol, but at the same time it would decrease the efficiency of the engine at high loads. It was found in the simulations that retarding spark from MBT timing by 5 and 10 crank angles after MBT timing leads to relative efficiency drops of approximately 1.5 and 4 respectively.

10.6. Autonomie Results

Nine performance maps were generated corresponding to three compression ratios (9.2, 11.5 and 13.5) and three spark retard limits applied during light knock (MBT, retarded up to 5 crank angle degrees and retarded up to 10 crank angle degrees). Each map was run using three drive cycles, UDDS, HWFET and US06.

Effect of Compression Ratio: It was found that increasing compression ratio from 9.2 to 13.5 increases the miles per gallon of the drive cycle by 2 to 6 percent depending on the drive cycle. The highest miles per gallon increase, in gasoline equivalent, was with the US06 cycle; about 5.7%. The smallest increase was with the UDDS cycle, 2.2%. This is lower than the engine efficiency gain seen during part load.

Miles traveled per gallon of ethanol used was significantly higher than the gasoline value, ranging from 141 miles per gallon of ethanol upward. Some of the low compression ratio cases with spark retard required no ethanol because spark retard raised the knock onset lines above the maximum torque of the drive cycle.

Effect of Spark Retard: Spark retard was introduced by dividing the performance map into three regimes; MBT timing, retarded spark timing. MBT timing was used at loads low enough that no ethanol was needed to prevent knock. Once knock onset was reached for UTG91, rather than add ethanol, the spark timing was retarded up to a limit in crank angles after MBT timing. Once the limit of spark retard was reached, ethanol was added and the spark was retarded at the limit. This strategy increased the miles traveled per gallon of ethanol used by a factor of 2 to 6 since less ethanol was needed to suppress knock with retarded timing.

10.7. Dependence of Knock Onset on Speed

When comparing the knock onset lines in simulation to experimental results it was determined that the experimental knock onset was less dependent on speed than the auto-ignition model would suggest. It was determined that, experimentally, the BMEP where knock onset occurs

was essentially independent of speed. This was attributed to the fact that knock onset can occur slightly later than at the peak pressure point in the course of combustion. By delaying the point of knock onset it was determined that, in the 1500 RPM to 3000 RPM range, extending the window of knock onset by 5 crank angle degrees after crank angle of peak pressure was more than enough to create a level knock onset lines.

Experimentally it was determined that it is possible for knock onset to occur later than peak pressure. By averaging over several knocking cases it was determined that it is possible for knock onset to occur up to seven crank angle degrees after peak pressure. This is the likely explanation of the discrepancy between the experiment and the simulation and makes horizontal knock onset lines plausible.

10.8. Future Work

Knock Onset: The auto-ignition integral was used to solve for the octane number of different fuels tested in the engine, and the octane number was then used to predict knock in cases beyond what could be simulated. This was effective at low speeds by assuming knock onset occurs at peak pressure, but at high speeds the model overestimated the load at which knock onset occurs. A more accurate auto–ignition model must therefore be developed to take into account the fact that knock onset can be delayed at higher speeds.

Engine Downsizing: Engine downsizing has the potential to yield efficiency gains, by taking advantage in the relative changes of different efficiency loss mechanisms. When increasing the compression ratio from 9.2 to 13.5, for example, the maximum BMEP of the engine increased by 1.41%. This means that, assuming the torque required out of the engine is the same, the engine could be downsized by 1.41%. This would give about 1.41% less friction increasing the efficiency of the overall engine.

Variables in the Simulation: The simulations only included constraints due to knock. In reality other constraints limit the engine performance, such as: peak pressure in the cylinder, turbine exit temperature, etc. Peak pressure at MBT reached almost 180 bars at the highest compression ratio studied here. This was much higher than the limit of our experimental turbocharged engine of 100 bars. A future study will include these additional limitations when generating performance maps.

References

[1] Heywood, J.B., Internal Combustion Engine Fundamentals, McGraw-Hill, 1988.

[2] Kasseris, E. and Heywood, J., "Charge Cooling Effects on Knock Limits in SI DI Engines Using Gasoline/Ethanol Blends: Part 1-Quantifying Charge Cooling," SAE Technical Paper 2012-01-1275, 2012, doi:10.4271/2012-01-1275.

[3] Douaud, A. and Eyzat, P., "Four-Octane-Number Method for Predicting the Anti-Knock Behavior of Fuels and Engines," SAE Technical Paper 780080, 1978, doi:10.4271/780080.

[4] Anderson, J., Leone, T., Shelby, M., Wallington, T. et al., "Octane Numbers of Ethanol-Gasoline Blends: Measurements and Novel Estimation Method from Molar Composition," SAE Technical Paper 2012-01-1274, 2012, doi:10.4271/2012-01-1274.

[5] Ayala, F., Gerty, M., and Heywood, J., "Effects of Combustion Phasing, Relative Air-fuel Ratio, Compression Ratio, and Load on SI Engine Efficiency," SAE Technical Paper 2006-01-0229, 2006, doi:10.4271/2006-01-0229.

[6] Grabner, P., Eichlseder, H., and Eckhard, G., "Potential of E85 Direct Injection for Passenger Car Application," SAE Technical Paper 2010-01-2086, 2010, doi:10.4271/2010-01-2086.

[7] Muranaka, S., Takagi, Y., and Ishida, T., "Factors Limiting the Improvement in Thermal Efficiency of S. I. Engine at Higher Compression Ratio," SAE Technical Paper 870548, 1987, doi:10.4271/870548.

[8] Jung, H., Leone, T., Shelby, M., Anderson, J. et al., "Fuel Economy and CO₂ Emissions of Ethanol-Gasoline Blends in a Turbocharged DI Engine," SAE Int. J. Engines 6(1):422-434, 2013, doi:10.4271/2013-01-1321.

[9] Muñoz, R., Han, Z., VanDerWege, B., and Yi, J., "Effect of Compression Ratio on Stratified-Charge Direct- Injection Gasoline Combustion," SAE Technical Paper 2005-01-0100, 2005, doi:10.4271/2005-01-0100.

[10] EPA, "Dynamometer Drive Schedules | Testing & Measuring Emissions | US EPA," 6 February 2013. <http://www.epa.gov/nvfel/testing/dynamometer.htm>

[11] Berry, I. M., "The Effects of Driving Style and Vehicle Performance on the Real-World Fuel Consumption of U.S. Light-Duty Vehicles," Master of Science Thesis,Massachusetts Institute of Technology, 2007.

[12] Toyota Website, "Features & Specs," Toyota Camry 2013, 2013, Web, <http://www.toyota.com/camry/features.html#!/mpg/2514/2532/2546/2540>